The University of
Nottingham

UNITED KINGDOM · CHINA · MALAYSIA

Panizzo, Virginia and Swann, George E.A. and Mackay, Anson W. and Vologina, Elena and Alleman, L. and Andre, L. and Pashley, Vanessa and Horstwood, Matthew S.A. (2017) Constraining modern day silicon cycling in Lake Baikal. Global Biogeochemical Cycles, 31 (3). pp. 556-574. ISSN 1944-9224

Access from the University of Nottingham repository:
http://eprints.nottingham.ac.uk/41075/8/Panizzo_et_al-2017-Global_Biogeochemical_Cycles.pdf

Copyright and reuse:

A note on versions:

The version presented here may differ from the published version or from the version of record. If you wish to cite this item you are advised to consult the publisher's version. Please see the repository url above for details on accessing the published version and note that access may require a subscription.

For more information, please contact eprints@nottingham.ac.uk

RESEARCH ARTICLE

Constraining modern-day silicon cycling in Lake Baikal

V. N. Panizzo[1,2] , G. E. A. Swann[1,2] , A. W. Mackay[3] , E. Vologina[4], L. Alleman[5], L. André[6], V. H. Pashley[7] , and M. S. A. Horstwood[7]

[1]School of Geography, University of Nottingham, University Park, Nottingham, UK, [2]Centre for Environmental Geochemistry, University of Nottingham, University Park, Nottingham, UK, [3]Environmental Change Research Centre, Department of Geography, University College London, London, UK, [4]Institute of Earth's Crust, Siberian Branch of the Russian Academy of Sciences, Irkutsk, Russia, [5]SAGE-Département Sciences de l'Atmosphère et Génie de l'Environnement, IMT Lille Douai, University of Lille, Lille, France, [6]Earth Sciences Department, Royal Museum for Central Africa, Tervuren, Belgium, [7]NERC Isotope Geosciences Laboratory, British Geological Survey, Nottingham, UK

Abstract Constraining the continental silicon cycle is a key requirement in attempts to understand both nutrient fluxes to the ocean and linkages between silicon and carbon cycling over different time scales. Silicon isotope data of dissolved silica ($\delta^{30}Si_{DSi}$) are presented here from Lake Baikal and its catchment in central Siberia. As well as being the world's oldest and voluminous lake, Lake Baikal lies within the seventh largest drainage basin in the world and exports significant amounts of freshwater into the Arctic Ocean. Data from river waters accounting for ~92% of annual river inflow to the lake suggest no seasonal alteration or anthropogenic impact on river $\delta^{30}Si_{DSi}$ composition. The absence of a change in $\delta^{30}Si_{DSi}$ within the Selenga Delta, through which 62% of riverine flow passes, suggests a net balance between biogenic uptake and dissolution in this system. A key feature of this study is the use of $\delta^{30}Si_{DSi}$ to examine seasonal and spatial variations in DSi utilization and export across the lake. Using an open system model against deepwater $\delta^{30}Si_{DSi}$ values from the lake, we estimate that 20–24% of DSi entering Lake Baikal is exported into the sediment record. While highlighting the impact that lakes may have upon the sequestration of continental DSi, mixed layer $\delta^{30}Si_{DSi}$ values from 2003 and 2013 show significant spatial variability in the magnitude of spring bloom nutrient utilization with lower rates in the north relative to south basin.

1. Introduction

Silicon isotope geochemistry (^{28}Si, ^{29}Si, and ^{30}Si) represents a growing field by which to constrain the global silicon cycle. The global silicon (Si) cycle is essentially characterized by two subcycles: the continental and oceanic silicon cycles, which are connected via regional river systems. Continental silicate-rock chemical weathering is responsible for the release of silicon into its dissolved phase (DSi), as orthosilicic acid (Si(OH)$_4$). DSi from soil solutions is ultimately precipitated into amorphous silica in plant tissue (phytoliths) or, via its transportation in rivers and lakes, by diatoms and sponges. The supply of DSi to the oceans by rivers plays a fundamental role in global biogeochemical cycling (dominated by siliceous phytoplankton; diatoms), which is responsible in part for the regulation of atmospheric pCO$_2$ [*Tréguer and Pondaven*, 2000].

Over the past decade a growing number of studies have employed $\delta^{30}Si_{DSi}$ methods in locations including the Amazon [*Hughes et al.*, 2013], Congo [*Cardinal et al.*, 2010; *Hughes et al.*, 2011a], Ganges [*Fontorbe et al.*, 2013; *Frings et al.*, 2015], Icelandic Rivers [*Georg et al.*, 2007; *Opfergelt et al.*, 2013], Nile [*Cockerton et al.*, 2013], Okavango Delta [*Frings et al.*, 2014a], Tana [*Hughes et al.*, 2012], Yangtze [*Ding et al.*, 2004], and Yellow [*Ding et al.*, 2011] drainage basins. Results from these have highlighted the close interactions between aquatic productivity and silicon cycling in both soils, vegetation, and other aboitic processes. However, relatively few have examined holistic changes in the terrestrial silicon cycle, despite the role these systems play in regulating silicon transportation into the ocean [*Tréguer et al.*, 1995; *Conley*, 2002; *Opfergelt and Delmelle*, 2012; *Tréguer and De La Rocha*, 2013; *Conley and Carey*, 2015; *Frings et al.*, 2016]. A recent review by *Frings et al.* [2016] addresses the extent to which variability in DSi transport over glacial and interglacial time scales, as a response to changes in climate, terrestrial vegetation type/cover, and hydrology [*Georg et al.*, 2006a; *Street-Perrott and Barker*, 2008], can be propagated to the ocean record [*Frings et al.*, 2016, and examples therein]. Such implications are particularly noted for large river reaches, where the effects of anthropogenic impacts and/or climate change can be notable. Here we present a detailed spatial study of the Lake Baikal catchment, in central Siberia, in order to examine the effects of some of these issues
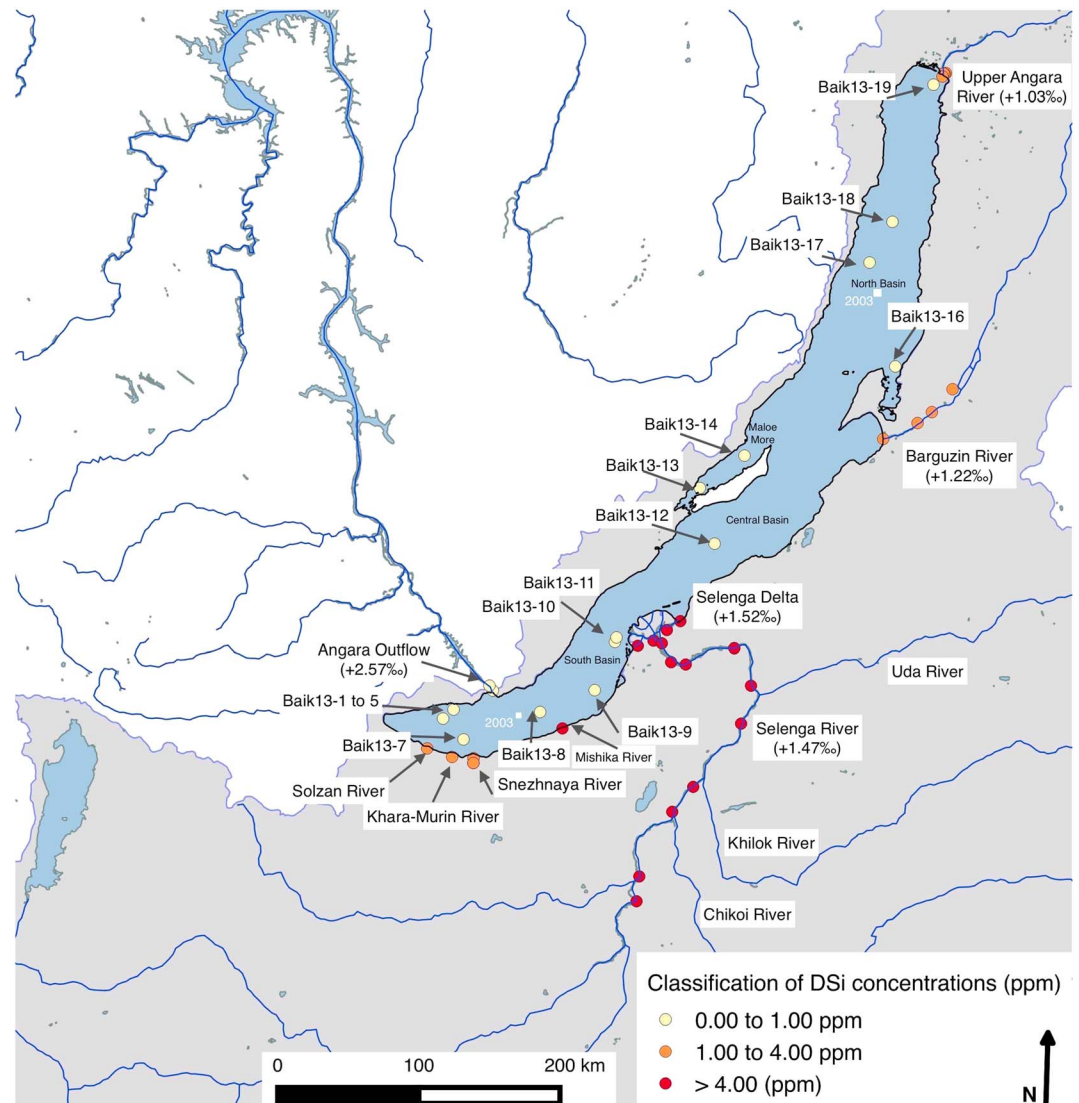
Figure 1. Map of Lake Baikal showing location of river and lake water samples collected in 2003 (white square symbol) and 2013 (circle symbol). River and lake water sample locations for 2013 data are color coded yellow, orange, and red according to their respective summer 2013 DSi concentrations (see legend). Mean $\delta^{30}Si_{DSi}$ (‰) data are displayed for the river inflows and correspond to mean values displayed for the respective river reach in Table 3. All site locations correspond to data presented in Tables 1–3. Figure was generated by using *QGIS Development Team* [2016] with data sets derived from *Digital Chart of the World* [2007], *Swiercz* [2007], and *Wessel and Smith* [2007].

(namely, catchment responses to climate warming and nutrient loading to the lake) upon long-term, and seasonal, nutrient (DSi) availability in the water column. We outline the rational for this research below.

1.1. An Introduction to Lake Baikal

Situated in one of the most continental regions of the world in central Siberia (Figure 1), Lake Baikal (103°43′–109°58′E and 51°28′–55°47′N) is the world's oldest, deepest, and most voluminous lake containing one fifth of global freshwater not stored in glaciers and ice caps [*Gronskaya and Litova*, 1991; *Sherstyankin et al.*, 2006]. Accordingly, the system is a major freshwater resource with its outflow ultimately entering the Yenisei River, the largest riverine inflow to the Arctic Ocean. Divided into three basins (south, central (including Maloe More), and north), separated by the Buguldeika Ridge running north-easterly from the shallow waters of the Selenga Delta and the Academician Ridge, respectively (Figure 1), the lake is characterized by a the high degree of endemic biodiversity [*Timoshkin*, 1997]. This endemicity has been attributed to the

lake's age and fully oxygenated water column, driven by seasonal overturning and deepwater renewal [*Weiss et al.*, 1991; *Shimaraev et al.*, 1994; *Wüest et al.*, 2005].

While overturning sustains a deepwater fauna that is almost entirely endemic to the lake [*Fryer*, 1991], the process also provides an important means of returning nutrients to the surface water [*Callender and Granina*, 1997]. This is a key driver in lake biogeochemical cycling which starts annually with under-ice diatom blooms in spring when ice/snow thickness permits photosynthesis [*Straškrábová et al.*, 2005; *Jewson et al.*, 2009]. The availability of DSi is a critical factor in regulating productivity including the formation of diatom frustules [*Martin-Jézéquel et al.*, 2000], which alongside picoplankton, dominate primary productivity in the lake. In instances of DSi limitation (unlike nitrogen and phosphorous), diatom cell wall formation is incomplete, cell division is impeded and the period of growth reduced [*Martin-Jézéquel et al.*, 2000].

While waters in Lake Baikal have a residency time of 377–400 years [*Gronskaya and Litova*, 1991], the residency time of DSi is shorter at 100–170 years [*Falkner et al.*, 1997; *Shimaraev and Domysheva*, 2004] due to biomineralization. Indeed, DSi residency in Lake Baikal can decrease by a factor of 5 when diatom productivity is increased [*Shimaraev and Domysheva*, 2004] or even be exhausted in summer surface waters following exceptionally high diatom blooms [*Jewson et al.*, 2010]. As such, the flux of DSi to the mixed layer (defined here as the surface), dominated by fluvial inputs to the lake and the upwelling of deepwater masses, plays a key role in maintaining Lake Baikal's unique ecosystem.

Here we use records of dissolved silicon and its silicon isotope composition ($\delta^{30}Si_{Dsi}$) to understand and model the transportation and fate of silicon through its dominant river tributaries and within biogeochemical cycling in Lake Baikal itself. With clear evidence for global anthropogenic perturbation of the continental silicon cycle [*Laruelle et al.*, 2009] and evidence of activities including urbanization, deforestation, agriculture, and mining around the lake [*Ciesielski et al.*, 2006], there is also an urgent need to assess whether rivers, flowing into Lake Baikal, show alterations related to major conurbations and/or other anthropogenic activity. The necessity for such work is emphasized by increasing evidence that the hydrology, chemistry, and biology of Lake Baikal are altering in response to a warmer climate [*Shimaraev and Domysheva*, 2013; *Izmest'eva et al.*, 2016]. Summer lake surface water temperatures have increased 2.4°C over the past ~60 years [*Hampton et al.*, 2008; *Shimaraev and Domysheva*, 2013] in tandem with evidence of later ice on and earlier ice off periods, particularly in the lake's southern basin [*Todd and Mackay*, 2003; *Hampton et al.*, 2008]. The effect of these two parameters has been to alter the thermal structure of Lake Baikal, which in turn has changed the spatial patterns of phytoplankton biomass across the lake [*Fietz et al.*, 2005; *Hampton et al.*, 2014]. The knock on effect of these trends, upon nutrient availability in the surface water column and the progression of diatom bloom development (via the mechanisms outlined above), has to date not been quantitatively assessed.

1.2. Characteristics of DSi Supply in Lake Baikal
1.2.1. Mixed Layer DSi Supply From Riverine Inputs

The catchment around Lake Baikal extends to an area of over 540,000 km^2 containing more than 350 rivers. These rivers play a key role in determining the hydrology and geochemistry of the lake by delivering ~83% of all water that enters the water column, with the remainder originating from direct precipitation and groundwater inflow [*Shimaraev et al.*, 1994]. Input, however, is strongly dominated by the three largest rivers with the Selenga River, extending southward into Mongolia, and the Upper Angara and Barguzin Rivers, draining the north of the catchment, contributing approximately 62%, 17%, and 8% of riverine inputs, respectively [*Seal and Shanks*, 1998] (Figure 1). Similarly, water loss from the lake is dominated by riverine flow with ~81% lost via the Angara River, the only outflow from the lake, and ~19% via evaporation [*Shimaraev et al.*, 1994].

The extreme continentality of the region exerts a major control on river flow through the seasonal interplay between the winter Siberian High and summer westerlies [*Lydolph*, 1977]. Whereas the Siberian High is responsible for the region's cold and dry winters, characterized by extensive ice cover on the lake from October to May (north basin) and January to April (south basin), the summer westerlies deliver approximately 70–90% of annual precipitation to the region [*Afanasjev*, 1976; *Shimaraev et al.*, 1994]. This seasonality has a corresponding impact on the timing of fluvial inputs to the lake with peak inflow in June, July, and August (JJA) and negligible inputs in January, February, and March. This is particularly noted for the Selenga River, the largest tributary, which has up to 80% of its annual input during JJA [*Sorokovikova et al.*, 2006].

Riverine inputs represent the primary source of silicon to the lake (312 mmol m^{-2} yr^{-1}) [*Callender and Granina*, 1997]. These inputs are low, however, compared to internal cycling within Lake Baikal [*Müller et al.*, 2005]: net sedimentation of silicon in the south basin has been estimated at 1170 mmol m^{-2} yr^{-1} while upwelling of deep waters to the surface is 630 mmol m^{-2} yr^{-1} [*Müller et al.*, 2005]. These estimations are based on two sites alone in the south and north basins of Lake Baikal.

With limnological and biogeochemical responses to climate change manifesting differently across (and within) the three basins of Lake Baikal (section 1.1), we propose the application of stable silicon isotope geochemistry to quantify spatial trends in DSi availability/demand more fully, with the technique acting as a tracer of biological demand by diatoms. This will enable both seasonal (spring and autumn) and long-term export estimations at a greater spatial resolution than was available before. Such examples are crucial for the later application of palaeolimnological approaches to compare with these contemporary estimates and therefore assess water column and biogeochemical responses to climate and human pressures in Lake Baikal.

1.2.2. Deepwater Nutrient Renewal

Lake Baikal's water column has a maximum depth of ~1642 m [*Troitskaya et al.*, 2014] and can be perceived as having two differing water masses. In surface waters down to the mesothermal maximum (MTM) (200–300 m water depth) convective mixing [*Shimaraev et al.*, 1994] and wind forced convection [*Troitskaya et al.*, 2014] generate overturning in spring and autumn and so influence mixed layer (namely, surface) nutrient supply. Below this, waters in the lake are permanently stratified [*Ravens et al.*, 2000; *Shimaraev et al.*, 1994; *Shimaraev and Granin*, 1991], although the supply of DSi to surface waters is dominated by convective mixing from depths below the MTM [*Shimaraev and Domysheva*, 2004].

Possible mechanisms for deepwater nutrient renewal include thermobaric instability on thermal bar regions (e.g., littoral regions) [*Shimaraev et al.*, 1993, 1994; *Killworth et al.*, 1996; *Wüest et al.*, 2005] and salinity differences either in the water column or arising from river inflows to the lake [*Hohmann et al.*, 1997; *Kipfer and Peeters*, 2000]. In either case, pelagic upwelling in Lake Baikal may last for up to 35 days, with a focus on the north eastern part of the South Basin, close to the Selenga Delta (Figure 1), and in the interval after summer stratification when the zonal depth of water movement increases from 80–100 m to 400–600 m [*Shimaraev et al.*, 2012]. The importance of this process in supplying nutrients to the mixed layer originates from water profiles showing higher DSi concentrations with depth, reflecting the remineralization/dissolution of amorphous silica as it sinks through the water column [*Weiss et al.*, 1991; *Killworth et al.*, 1996; *Falkner et al.*, 1997; *Shimaraev and Domysheva*, 2004]. For example, south basin data from 1994 to 2001 show higher DSi concentrations at 300–1400 m than surface waters [*Weiss et al.*, 1991; *Killworth et al.*, 1996; *Shimaraev and Domysheva*, 2004; *Shimaraev et al.*, 2012] with remineralization estimated to recharge surface waters by up to 630 mmol m^{-2} yr^{-1} [*Müller et al.*, 2005]. This work helps to elucidate the inherent complexity of DSi cycling in Lake Baikal, which has been raised in previous studies [*Müller et al.*, 2005], by using silicon isotope geochemistry to provide a more robust spatial and temporal interpretation of DSi utilization and deepwater export across the lake. This is due to the ability of δ^{30}Si$_{DSi}$ approaches to act as a tracer of diatom utilization in Lake Baikal, permitting a more robust estimation of south, central, and north basin spring and autumn bloom DSi utilization. The application of this method is also further acknowledged as comparison with data presented here permits the ability to later apply palaeolimnological (δ^{30}Si$_{diatom}$) approaches (as validated by *Panizzo et al.* [2016]) to quantify impacts on biogeochemical cycling as a response to climate change and nutrient loading in Lake Baikal.

2. Methods

2.1. Sample Locations

The data in this manuscript primarily originate from four expeditions to Lake Baikal and the surrounding region in 2003, 2013, and 2014 (Figure 1). The winter (February–March) 2013 lake water δ^{30}Si$_{DSi}$ compositions at one site (BAIK13-1) and a number of summer 2013 water δ^{30}Si$_{DSi}$ data from across the lake have previously been reported by *Panizzo et al.* [2016] (winter data). These results are summarized alongside new snow, ice, lake, and river δ^{30}Si$_{DSi}$ data and results from expeditions to Lake Baikal in 2003 and 2014 (see Tables 1–3 for full details).

2.1.1. Lake Samples

An expedition to Lake Baikal in July 2003, funded by European Union CONTINENT program (EVK2-CT-2000-0057), resulted in water column profiles of δ^{30}Si$_{DSi}$ being collected at a site in the south (105.0321°E,

Table 1. July 2003 Water Profile Data From the South and North Basins Along With Respective Location Sampling of Lake Baikal[a]

Water Column Depth (m)	DSi (ppm)	$\delta^{29}Si_{DSi}$ (‰)	Uncertainty (1σ)	$\delta^{30}Si_{DSi}$ (‰)
South Basin (105.0321°E, 51.71282°N)				
10	0.57	+1.16	0.04	+2.23
25	0.61	+1.18	0.03	+2.28
50	0.60	+1.17	0.01	+2.26
100	0.56	+1.09	0.02	+2.10
150	0.57	+1.07	0.03	+2.07
250	0.56	+1.07	0.01	+2.06
500	0.83	+0.92	0.08	+1.77
750	1.06	+0.95	0.05	+1.83
1000	1.22	+0.85	0.08	+1.65
1200	1.24	+0.90	0.03	+1.73
1400	0.85	+0.83	0.04	+1.59
North Basin (109.0051°E, 54.4438°N)				
5	0.84	+1.11	0.04	+2.13
15	0.83	+1.18	0.02	+2.27
25	0.89	+0.97	0.01	+1.88
50	0.84	+1.01	0.08	+1.96
100	0.84	+1.01	0.03	+1.95
150	0.82	+0.99	0.07	+1.90
250	0.87	+1.04	0.03	+2.01
500	1.05	+0.93	0.03	+1.80
750	1.23	+0.87	0.06	+1.68
850	1.36	+0.94	0.04	+1.82

[a]$\delta^{30}Si_{DSi}$ is calculated as $\delta^{29}Si = 0.518 \cdot \delta^{30}Si$ due to the mass-dependent fractionation between the ratios of the isotopes. Reproducibility for $\delta^{30}Si_{DSi}$ is estimated at 0.14‰ by similarly applying the same calculation. Data are presented in Figure 2.

51.71282°N) and north basins (109.0051°E, 54.4438°N) aboard the R/V *Vereshagin* at water depths of 5-1400 m (Table 1). Samples were stored in 4 L acid-washed high-density polyethylene bottles ready for their return to the laboratory.

Further summer waters from the mixed layer (mixed layer water depth: $\bar{x} = 6.66$ m, $1\sigma = \pm4.79$ m) of Lake Baikal were collected at a depth of 1 m in August 2013 with sampling across all three basins of the lake including sites close to the inflow of the Khara-Murin and Snezhnaya Rivers and sites ~1.8 km offshore of the Selenga Delta (Table 2 and Figure 1). Only surface water data are provided in Table 2 as these samples capture the mean mixed layer across the lake.

These samples were complemented by an expedition to the south basin of the lake in February–March 2013 when (1) fluvial inflows and precipitation to the lake are minimal [*Afanasjev*, 1976; *Seal and Shanks*, 1998] and (2) there is minimal photosynthetic activity/diatom biomineralization, the latter of which was confirmed by no/negligible chlorophyll *a* in waters down to 200 m depth [*Panizzo et al.*, 2016]. Averages of the profile data are therefore provided for the purpose of this manuscript (Table 2), where we assume the absence of biological uptake and surface water mixing (collection below ice). Lake water $\delta^{30}Si_{DSi}$ values were collected at three sites in the south basin (BAIK13-1, BAIK13-4, and BAIK13-5; Figure 1 and Table 2), also sampled in August 2013, using a 2 L Van Dorn sampler at depths from 1 to 180 m. Samples were collected from BAIK13-1 on two occasions 9 days apart (BAIK13-1a and BAIK13-1b) to assess short-term temporal variations in $\delta^{30}Si_{DSi}$. In addition, one lake surface snow sample and one lake ice sample were collected from BAIK13-1 (Table 2).

2.1.2. River Samples

In August 2013 samples were collected from the wider drainage basin around Lake Baikal at the time of peak river flow [*Afanasjev*, 1976; *Seal and Shanks*, 1998] (Figure 1 and Table 3). This involved sampling rivers that supply up to 92% of the total annual riverine inflow to the lake [*Seal and Shanks*, 1998], including the Selenga, Upper Angara, Barguzin, Snezhnaya, Mishika, Khara-Murin, and Solzan Rivers, using a modified bottle sampler attached to a rope in order to sample as close as possible to the central region of the river channel. Of the sampled rivers, the Upper Angara flows into the north basin, the Barguzin River into the central basin, and the remainder into the south basin of the lake. To account for seasonal variability in

Table 2. DSi, $\delta^{30}Si_{DSi}$, and $\delta^{29}Si_{DSi}$ Lake Water Data at Sites in Lake Baikal Sampled in 2013 Together With Respective Uncertainties[a]

Site	Location	Longitude	Latitude	DSi (ppm)	$\delta^{30}Si_{DSi}$ (‰)	Uncertainty (2σ)	$\delta^{29}Si_{DSi}$ (‰)	Uncertainty (2σ)
Winter (February/March) 2013 Lake Waters								
BAIK13-1	South basin—snow sample	104.41611°E	51.76778°N	0.04	BDL	BDL	BDL	BDL
BAIK13-1	South basin—lake ice sample	104.41611°E	51.76778°N	0.01	BDL	BDL	BDL	BDL
BAIK13-1a[b]	South basin ($\bar{x}$ upper 180 m)	104.41611°E	51.76778°N	1.07	+2.31	0.29[c]	+1.23	0.09[c]
BAIK13-1b[b]	South basin ($\bar{x}$ upper 50 m)	104.41611°E	51.76778°N	1.06	+2.29	0.23[c]	+1.19	0.10[c]
BAIK13-4[b]	South basin ($\bar{x}$ upper 180 m)	104.30003°E	51.69272°N	0.91	+2.23	0.26[c]	+1.21	0.20[c]
BAIK13-5[b]	South basin ($\bar{x}$ upper 180 m)	104.27411°E	51.65053°N	0.93	+2.30	0.24[c]	+1.19	0.18[c]
Summer (August) 2013 Lake Waters								
BAIK13-1	South basin	104.41611°E	51.76778°N	0.62	+2.97	0.17	+1.36	0.07
BAIK13-4	South basin	104.30003°E	51.69272°N	0.66	+2.49	0.20	+1.27	0.13
BAIK13-5	South basin	104.29125°E	51.64708°N	0.66	+2.39	0.14	+1.22	0.06
BAIK13-7	South basin	104.52861°E	51.56833°N	0.69	+2.47	0.15	+1.32	0.08
BAIK13-8	South basin	105.31456°E	51.74386°N	0.65	+2.42	0.25	+1.21	0.11
BAIK13-9	South basin	105.87786°E	51.88053°N	0.69	+2.18	0.22	+1.14	0.13
BAIK13-10	South basin	106.09389°E	52.18528°N	0.68	+2.30	0.16	+1.29	0.07
BAIK13-11	South basin	106.11017°E	52.21361°N	0.35	+3.18	0.20	+1.66	0.09
BAIK13-12	Central basin	107.15800°E	52.79814°N	0.13	+2.84	0.27	+1.41	0.16
BAIK13-13	Central basin (Maloe More)	107.01880°E	53.15600°N	0.70	+2.40	0.15	+1.27	0.06
BAIK13-14	Central basin (Maloe More)	107.50480°E	53.35167°N	0.66	+2.33	0.17	+1.28	0.07
BAIK13-16	North basin	109.16472°E	53. 87528°N	0.49	+2.53	0.17	+1.27	0.08
BAIK13-17	North basin	108.95028°E	54.54442°N	0.87	+2.21	0.22	+1.14	0.10
BAIK13-18	North basin	109.22690°E	54.79536°N	0.87	+2.02	0.12	+1.07	0.05
BAIK13-19	North basin	109.78270°E	55.64939°N	0.93	+1.74	0.14	+0.90	0.05
Delta_22	1.8 km from Selenga Delta	106.22167°E	52.26722°N	2.80	+1.67	0.11	+0.83	0.06
Delta_23	1.8 km from Selenga Delta	106.21472°E	52.22361°N	3.31	+1.61	0.11	+0.79	0.06
B13_8_2	Nr. Khara-Murin River outflow	104.15523°E	51.52934°N	0.92	+1.95	0.12	1.03	0.07
B13_8_4	Nr. Vydrino River outflow	104.64550°E	51.47618°N	0.81	+2.16	0.12	1.14	0.07

[a]Winter samples are profile means of sampled waters above the MTM (200 m water depth). Duplicate winter samples from BAIK13-1 (BAIK13-1a and BAIK13-1b) were collected 9 days apart, with the latter to between a water depth of 0–50 m. All summer samples are from 1 m water depth alone. With the mean summer mixed layer depth at 6.66 m (1σ = ±4.79 m) deeper DSi and $\delta^{30}Si_{DSi}$ data are not included due to the potential for values to be altered by diatom dissolution during sinking (refer to section 1.2 for full explanation).
[b]Results published in *Panizzo et al.* [2016].
[c]Errors are 2 SD of the average values.

river flow a sample was also collected below ice in the Selenga River in spring 2014 (Table 3). Samples in August 2013 were also collected from (1) the Selenga Delta ($n = 8$), a large wetland of 540 km² [*Fefelov*, 2001] through which the Selenga River drains before entering the lake (Figure 1 and Table 3), and (2) the Angara River ($n = 2$) outflow (Table 3).

2.2. Analytical Methods
2.2.1. 2003 Field Season Samples
Water samples collected in 2002 were filtered through 0.4 μm polycarbonate filters on return to the laboratory (the Royal Museum for Central Africa, Tervuren) before being processed according to the procedures outlined in *Cardinal et al.* [2005] for isotopic analyses. Si isotopic measurements were carried out in 2005 at Université Libre de Bruxelles (ULB) under dry plasma conditions (Aridus desolvator) by using a Nu Plasma multicollector-inductively coupled plasma-mass spectrometer (MC-ICP-MS), with a Mg external standard [see *Cardinal et al.*, 2003]. At that time, we measured and used exclusively the $\delta^{29}Si$ notation as the ^{30}Si signal was disturbed by isobaric interference on the low-resolution Nu Plasma instrument available at ULB [see *Cardinal et al.*, 2003]. The $\delta^{30}Si$ values have been calculated from $\delta^{29}Si$ assuming a theoretical terrestrial mass-dependent equilibrium fractionation slope between the two isotopes:

$$\delta^{29}Si = 0.518 \cdot \delta^{30}Si \left(R^2 = 0.851 \right) \tag{1}$$

As this prevents us from detecting any analytically induced mass-dependent fractionation processes between Si isotopes through a $\delta^{30}Si$ versus $\delta^{29}Si$ graph, we checked such bias daily (for independent analytical sessions) by using Mg versus Si isotope ratios on every National Bureau of Standards 28 bracketing standard. Based on this standard-sample bracketing technique, a few results with an unstable fractionation line were discarded (less than 10% of the whole data set) in addition to those samples that generally reflected unsteadiness in

Table 3. August 2013 DSi and $\delta^{30}Si_{DSi}$ and $\delta^{29}Si_{DSi}$ Data From Rivers Flowing Into and Out of Lake Baikal[a]

Location	Longitude	Latitude	DSi (ppm)	$\delta^{30}Si_{DSi}$ (‰)	Uncertainty (2σ)	$\delta^{29}Si_{DSi}$ (‰)	Uncertainty (2σ)
Selenga River 1 (Ilyinka)	107.32987°E	52.12787°N	4.48	+1.48	0.12	+0.82	0.06
Selenga River 2 (Tataurovo)	107.32989°E	52.12777°N	4.52	+1.50	0.11	+0.78	0.07
Selenga River 3 (Sotnikovo)	107.48936°E	51.88560°N	4.63	+1.50	0.11	+0.74	0.06
Selenga River 4 (Kolobki)	107.37460°E	51.64598°N	4.55	+1.50	0.13	+0.81	0.07
Selenga River 5 (Dede-Sutoy)	106.86765°E	51.25107°N	4.55	+1.49[c]	0.12[c]	+0.77[c]	0.10[c]
Selenga River 6 (Novoselenginsk)	106.64846°E	51.09519°N	4.63	+1.45	0.16	+0.73	0.06
Selenga River 7 (after Deben)	106.30345°E	50.68855°N	4.62	+1.42	0.12	+0.77	0.07
Selenga River 8 (Ust-Kyakhta)	106.27130°E	50.53031°N	4.85	+1.46	0.11	+0.76	0.06
Selenga River Mean			**4.60**	**+1.47**	**0.06**[b]	**+0.77**	**0.06**
Selenga Delta 1 (Murzino)	106.49386°E	52.18881°N	4.72	+1.31[c]	0.13[c]	+0.71[c]	0.11[c]
Selenga Delta 1 (Kabansk)	106.67223°E	52.05072°N	4.76	+1.55	0.12	+0.77	0.07
Selenga Delta 1 (Selenginsk)	106.82250°E	52.03369°N	4.85	+1.38	0.15	+0.74	0.10
Selenga Delta 1 (Kryasnyj Jar)	106.58006°E	52.17083°N	4.76	+1.56	0.16	+0.77	0.10
Selenga Delta 1 (Korsakovo)	106.63535°E	52.25459°N	6.30	+1.77[c]	0.11[c]	+0.93[c]	0.10[c]
Selenga Delta 1 (Dubinino)	106.77750°E	52.30956°N	4.72	+1.51	0.12	+0.77	0.07
Selenga Delta 1 ("Base camp")	106.32996°E	52.12787°N	4.51	+1.54	0.12	+0.80	0.06
Selenga Delta Mean			**4.95**	**+1.52**	**0.29**[b]	**+0.78**	**0.14**[b]
Solzan River	104.15848°E	51.50852°N	3.09	+0.94	0.18	+0.49	0.07
Khara-Murin River	104.41336°E	51.45571°N	3.67	+0.93	0.15	+0.48	0.10
Snezhnaya River 1	104.63248°E	51.44871°N	3.31	+1.01	0.12	+0.53	0.06
Snezhnaya River 2	104.63117°E	51.41781°N	3.30	+1.04	0.18	+0.55	0.08
Snezhnaya River 3	104.63118°E	51.41779°N	3.48	+0.90	0.16	+0.43	0.10
Snezhnaya River Mean			**3.36**	**+0.98**	**0.14**[b]	**+0.50**	**0.13**
Mishika River	105.54248°E	51.63849°N	4.13	+1.02[c]	0.13[c]	+0.53[c]	0.11[c]
Barguzin River 1 (Zorino)	109.36650°E	53.50640°N	3.11	+1.21	0.11	+0.61	0.06
Barguzin River 2	109.76355°E	53.70734°N	3.83	+0.99	0.12	+0.52	0.06
Barguzin River 3	109.52647°E	53.57019°N	3.04	+1.41	0.11	+0.70	0.07
Barguzin River 4	108.73846°E	54.61193°N	3.21	+1.25	0.11	+0.63	0.06
Barguzin River Mean			**3.30**	**+1.22**	**0.35**[b]	**+0.62**	**0.15**[b]
Upper Angara River 1	109.93114°E	55.71752°N	2.80	+1.10	0.14	+0.52	0.06
Upper Angara River 2	109.91707°E	55.71214°N	2.55	+0.90	0.17	+0.49	0.13
Upper Angara River 3	109.90556°E	55.71541°N	2.72	+1.02	0.10	+0.55	0.06
Upper Angara River 4	109.87991°E	55.87991°N	2.64	+1.09	0.13	+0.55	0.06
Upper Angara River Mean			**2.68**	**+1.03**	**0.06**[b]	**+0.53**	**0.07**[b]
Angara River 1	104.82733°E	51.88130°N	0.57	+2.55	0.11	+1.31	0.06
Angara River 2 (Reservoir, Irkutsk)	104.79253°E	51.91239°N	0.58	+2.59	0.12	+1.30	0.06
Angara River (outflow) Mean			**0.58**	**+2.57**	**0.05**[b]	**+1.31**	**0.00**[b]
Under ice Selenga River (Selenginsk)	106.87588°E	52.05631°N	5.52	+1.54	0.14	+0.77	0.10

[a]The under-ice Selenga River sample (March 2014) is also provided at the bottom of the table. Respective uncertainties are provided for all data. Values in bold correspond to mean values with 2 SD uncertainties (where $n > 1$) for each of the inflowing Lake Baikal rivers. Data are presented in Figures 3a and 3b.
[b]These errors are 2 SD of the average values.
[c]These data represent weighted averages of sample replicates. Errors are the 95% confidence of these values, incorporating the propagated long-term diatomite excess variance.

either the plasma or the dissolution system. A reproducibility test that included molybdate coprecipitation and isotopic analyses of 10 individual aliquots from a single seawater sample gave a standard deviation on the $\delta^{29}Si$ of 0.07‰ (2σ) [*Cardinal et al.*, 2005]. Through the application of equation (1), this equates to a reproducibility of 0.14‰ for $\delta^{30}Si$ (Table 1), which is comparable with long-term variance derived for 2013/2014 data analyzed at British Geological Survey (BGS) (section 2.2.2).

2.2.2. 2013/2014 Field Season Samples

Water samples collected for DSi concentration and $\delta^{30}Si_{DSi}$ analyses in 2013/2014 were filtered through 0.4 μm polycarbonate filters (Whatman) before storage in 125 mL acid-washed low-density polyethylene bottles. Samples were acidified with Romil Ultapure HCl (10 M) to a pH above 2 in order to preserve

samples until analysis in the UK. Silicon and trace metal concentrations on all samples were measured on an inductively coupled plasma–mass spectrometer (ICP-MS) (Agilent Technologies 7500) at the British Geological Survey. All DSi data are reported by ICP-MS in parts per million and where necessary values are converted to micromole for comparison with other studies.

Samples were purified by passing a known volume (between 1 and 2.5 mL depending on silicon concentration) through a 1.8 mL cationic resin bed (BioRad AG50W-X12) [*Georg et al.*, 2006b] and eluted with 3 mL of Milli Q water in order to obtain an optimal silicon concentration of between 3 and 10 ppm. Where samples (namely, March 2013 lake samples) were less than <1.5 ppm DSi, a preconcentration step was carried out, which is fully detailed in *Panizzo et al.* [2016]. Isotope analyses were made on a ThermoFisher Scientific Neptune Plus MC-ICP-MS (multicollector-inductively coupled plasma-mass spectrometer), in wet-plasma mode at the BGS. In order to overcome any analytical bias due to differing matrices, samples and reference materials were acidified by using HCl (to a concentration of 0.05 M, using Romil UPA) and sulphuric acid (to a concentration of 0.003 M, using Romil UPA). This was done following *Hughes et al.* [2011b], the principle being that doping samples and standards alike, above and beyond the natural abundance of Cl^- and SO_4^{2-}, will evoke a similar mass bias response in each. Finally, all samples and standards were doped with ~300 ppb magnesium (Mg, Alfa Aesar SpectraPure) ($^{24}Mg/^{25}Mg = 0.126633$) to correct the data for the effects of instrument induced mass bias [*Cardinal et al.*, 2003; *Hughes et al.*, 2011b; *Oelze et al.*, 2016]. Full details on machine instrumentation, sampling preparation, and blank procedures are provided in the supporting information S1 and additionally in *Panizzo et al.* [2016].

All uncertainties are reported at 2σ absolute and incorporate an excess variance derived from the diatomite validation material, which was quadratically added to the analytical uncertainty of each measurement. Please refer to supporting information S1 for further information on uncertainty calculations. Long-term (~2 years) variance for the method is as follows: diatomite = +1.23‰ ± 0.16‰ (2 SD, $n = 210$) (consensus value of +1.26‰ ± 0.2‰, 2 SD [*Reynolds et al.*, 2007]) and RMR4 = +0.88‰ ± 0.20‰ (2 SD, $n = 42$).

3. Results

3.1. Lake Samples

#### 3.1.1. Winter Sampling (February–March 2013)
Due to the very low concentration of DSi in the ice and snow samples from BAIK13-1 (<0.05 ppm; Table 2) isotopic analyses were not possible. Filtering (at 0.2 μm) up to 10 L of melted ice also yielded minimal diatom valves, suggesting that ice bound diatom populations in the lake are negligible at the time of sampling. Below ice lake water DSi concentrations from March 2013 in the south basin (0–180 m depth) range from 0.74 to 1.22 ppm with a mean $\delta^{30}Si_{DSi}$ for each site between 0 and 180 m water depth ranging from +2.23‰ to +2.31‰ (Table 2). Re-sampling at site BAIK13-1 9 days after the original sampling revealed no change in $\delta^{30}Si_{DSi}$ (BAIK13-1a and BAIK13-1b; Table 2).

3.1.2. Summer Sampling (July 2003)
Summer DSi concentrations in the south basin above the MTM (between 5 and 250 m water depth; $\bar{x} = 0.58$ pmm, 1 SD = 0.02 ppm) are significantly lower than the north basin (5–250 m water depth, $\bar{x} = 0.85$ pmm, 1 SD = 0.03 ppm) (Table 1 and Figure 2). In contrast deepwater (≥500 m water depth) concentrations are higher and within the range of variability of one another (south basin: $\bar{x} = 1.04$ ppm, 1 SD = 0.20 ppm; north basin: $\bar{x} = 1.21$ ppm, 1 SD = 0.16 ppm). In both basins $\delta^{30}Si_{DSi}$ signatures decrease through the water column with values of approximately +2.23 to +2.13‰ in the upper 10 m of the water column compared to mean deepwater (here defined as below 500 m) values of +1.71‰ (1 SD = 0.10‰) and +1.77‰ (1 SD = 0.08‰) in the south and north basins, respectively (Table 1).

3.1.3. Summer Sampling (August 2013)
Summer 2013 mixed layer (sampled water depth = 1 m) DSi values across the lake vary from 0.13 to 0.93 ppm, $\bar{x} = 0.64$ ppm, with typical values 0.49–0.93 ppm in the north basin and 0.62–0.70 ppm in the south/central basin. The exceptions to these trends are low concentrations of 0.35 ppm at BAIK13-11 in the South Basin and 0.13 ppm at BAIK13-12 in the central basin. $\delta^{30}Si_{DSi}$ compositions across the lake show a negative relationship to DSi data, with values ranging from +1.74‰ to +2.53‰ in the north basin ($\bar{x} = +2.13‰$, 1 SD = 0.33‰), >+2.30‰ in the central basin including Maloe More ($\bar{x} = +2.52‰$, 1 SD = 0.28‰), and up to +3.18‰ in south basin ($\bar{x} = 2.55‰$, 1 SD = 0.34‰) (Table 2 and Figure 1).
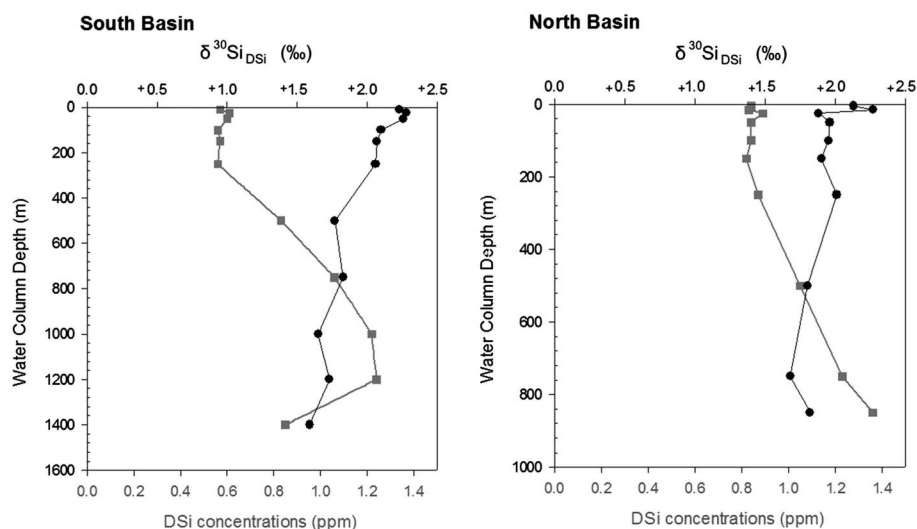
Figure 2. Summer 2003 profile data of DSi concentrations (ppm) (in grey) and $\delta^{30}Si_{DSi}$ (‰) (in black) compositions against water column depth (m) for the south and north basins of Lake Baikal. All data are derived from Table 1. Note that the analytical uncertainties for $\delta^{30}Si_{DSi}$ signatures are not plotted as data are derived from the conversion of ^{29}Si although reproducibility is estimated at 0.14‰ (see Table 1).

Lake waters ~1.8 km from the Selenga Delta outflow show the influence of riverine inputs with surface water DSi concentrations (2.80 ppm and 3.31 ppm) and $\delta^{30}Si_{DSi}$ compositions (+1.67‰ and +1.61‰) closer to values for the Selenga River/Delta than lake samples at open water locations (Delta 22 and Delta 23; see section 3.2 below and Table 2). In contrast, minimal riverine influence is detected in waters ~20 m from the inflow of the smaller Khara-Murin and Snezhnaya Rivers with values instead similar to other lake waters (DSi = 0.92 ppm, 0.81 ppm; $\delta^{30}Si_{DSi}$ = +1.95‰ and +2.16‰) (B13_8_2 and B13_8_4; Figure 1 and Table 2).

3.2. River/Catchment Samples

Summer samples from the Angara River, the only outflow from Lake Baikal, contain <1 ppm of DSi and are similar to summer 2003 and 2013 lake water values reported in sections 3.1.2 and 3.1.3 (Table 3). Summer DSi concentrations of all inflowing rivers are between 2.55 and 6.30 ppm (Table 3) including the Upper Angara River (2.68 ppm), Barguzin River (3.30 ppm), and the southern basin tributaries: Solzan (3.09 ppm), Khara-Murin (3.67 ppm), and the Snezhnaya (3.36 ppm) Rivers (Table 3). Concentrations in the Selenga River (4.48–4.85 ppm, $\bar{x}$ = 4.60 ppm, n = 8) and Selenga Delta (4.51–6.30 ppm, $\bar{x}$ = 4.95 ppm, n = 8) are consistently ~1 ppm more concentrated than other river inflows (Table 3 and Figure 1). Along the course of the Selenga River and Selenga Delta there is no clear variation in DSi, apart from one higher value near the village of Korsakovo of 6.30 ppm. An under-ice Selenga River value of 5.52 ppm from March 2014 is also higher than the mean summer 2013 average DSi concentration along the river (4.60 ppm).

From an isotope perspective, the Angara River outflow, sampled during summer months, has a relatively high value of approximately +2.58‰ that is similar to summer lake waters. In contrast, the $\delta^{30}Si_{DSi}$ signatures of all inflows range from +0.90‰ to +1.77‰ (Table 3 and Figure 1). Mean calculations were derived to summarize spatial variability in the tributaries where $n > 1$ (Table 3). Values for the Selenga, Barguzin, and Upper Angara Rivers are +1.47‰ ± 0.06 (2 SD, n = 8), +1.22‰ ± 0.35 (2 SD, n = 4), and +1.03‰ ± 0.06 (2 SD, n = 4), respectively. The assortment of other inflows sampled along the southern shore of Lake Baikal (Solzan, Khara-Murin, Snezhnaya, and Mishika Rivers, n = 7) are generally lower and within uncertainty of each other (+0.90‰ to +1.04‰) (Table 3). As with DSi concentrations, the $\delta^{30}Si_{DSi}$ compositions at Korsakovo are slightly higher (+1.77‰) than the remaining values for the Selenga River, including downstream sites (Selenga River mean = +1.47‰, 0.21 SD, n = 7). The $\delta^{30}Si_{DSi}$ signatures of waters in the Selenga Delta (+1.52‰ ± 0.29 2 SD, n = 8) are also similar to those of the Selenga River, as is the single winter $\delta^{30}Si_{DSi}$ composition collected from the Selenga River (+1.54‰ ± 0.14).
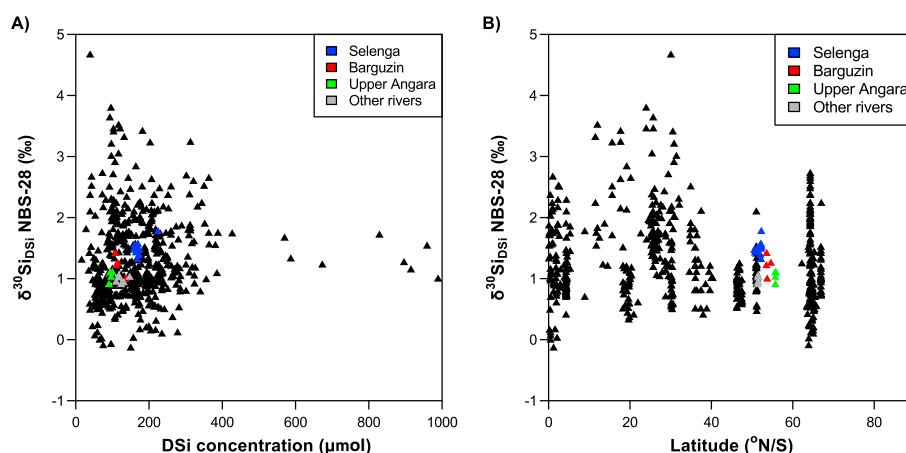
Figure 3. Global variations in river $\delta^{30}Si_{DSi}$ (‰) signatures against (a) DSi concentrations (μmol) and (b) latitude (°N/S) (black triangles) alongside values from rivers flowing into Lake Baikal (colored triangles—see legend). Global data set complied by *Frings et al.* [2016].

4. Discussion

4.1. Variations in $\delta^{30}Si_{DSi}$ Inflow to Lake Baikal

The $\delta^{30}Si_{DSi}$ compositions of rivers flowing into Lake Baikal fall within the range of other river systems across the globe, including sites impacted by humans (−0.9‰ to +4.7‰) [*De la Rocha et al.*, 2000; *Ding et al.*, 2004, 2011; *Alleman et al.*, 2005; *Ziegler et al.*, 2005a, 2005b; *Georg et al.*, 2006a, 2007; *Cardinal et al.*, 2010; *Engström et al.*, 2010; *Hughes et al.*, 2011a, 2012, 2013; *Opfergelt et al.*, 2011, 2013; *Cockerton et al.*, 2013; *Delvaux et al.*, 2013; *Fontorbe et al.*, 2013; *Pokrovsky et al.*, 2013; *Sun et al.*, 2013; *Frings et al.*, 2014a; *Mavromatis et al.*, 2016]. As such, these systems encompass a wide range of land uses, geology, vegetation, and climate, which all play an active role in driving river $\delta^{30}Si_{DSi}$ compositions. This work differs from previous studies, which have largely focused on main channel compositions and tributary mixing of $\delta^{30}Si_{DSi}$ signatures [e.g., *Ding et al.*, 2004; *Hughes et al.*, 2011b, 2012, 2013; *Cockerton et al.*, 2013; *Delvaux et al.*, 2013; *Fontorbe et al.*, 2013], by summarizing the main patterns in the riverine $\delta^{30}Si_{DSi}$ data before presenting an open system model (section 4.2) that incorporates fluvial fluxes of dissolved silicon to constrain the silicon cycle in Lake Baikal.

4.1.1. Seasonal Variations in Riverine Flow

Lake Baikal lies within the Yenisei drainage basin, the seventh largest in the world. Despite the different geology (basalt versus dominant granitoids around Lake Baikal) values in this study are similar to those recorded in the Kulingdakan River watershed approximately 500–1000 km north of Lake Baikal, but in the same basin [*Pokrovsky et al.*, 2013]. While the winter sample from the Selenga River is similar to summer Selenga River values, suggesting no seasonal variation in river $\delta^{30}Si_{DSi}$ (+1.54‰ ± 0.14 (winter); +1.48‰ ± 0.04 (summer)), an up to +1.5‰ decrease in $\delta^{30}Si_{DSi}$ was documented in the Kulingdakan watershed during spring ice melt [*Pokrovsky et al.*, 2013] and for the wider Yenisey drainage basin during permafrost melting (up to +1.75 and +2‰ heavier) [*Mavromatis et al.*, 2016]. Seasonal decreases have also been observed in rivers in northern Sweden [*Engström et al.*, 2010]. In both cases the decreases have been partially attributed to an increase in suspended load and in particular the dissolution of plant derived silicon which seasonally dominates the solid phase of silicon in surface soils, both of which act as pools enriched in the lighter ^{28}Si [*Engström et al.*, 2010; *Pokrovsky et al.*, 2013; *Mavromatis et al.*, 2016]. The lack of seasonal variation in the Selenga River could reflect the absence of seasonal biotic and abotic processes affecting $\delta^{30}Si_{DSi}$ signatures, potentially related to the larger size of the Selenga River, which may buffer any seasonal signal. In either case with (1) the Selenga River providing 62% of all riverine inflow to the lake and (2) the summer inflow of all rivers providing >75% of all riverine inputs to the lake, we suggest that our summer river $\delta^{30}Si_{DSi}$ data are representative of annual riverine inputs to Lake Baikal and so can be used to model lake water dynamics below in section 4.2.

4.1.2. Spatial Variations in the Selenga River

DSi concentrations for all Lake Baikal inflows range between 2.55 and 6.30 ppm (Table 3 and Figure 3a). These values lie comfortably within the range of other global river systems as well as rivers at these latitudes (Figures 3a and 3b) [*Frings et al.*, 2016]. With the main aim of this manuscript to model Lake Baikal

contemporary DSi cycling, a more in-depth discussion on the river inflow isotopic geochemistry is not provided here. However, an illustration of the data as an attempt to assess the degree of DSi removal via secondary mineral clay formation and/or biological uptake is provided for illustrative purposes in supporting information S2.

The Selenga River was sampled the most comprehensively out of the total seven rivers sampled in this study. The Selenga River reach (from waters close to the Mongolian border (Ust-Kyakhta) through to and including the Selenga Delta) contains some of the region's largest industrial centers along its banks. Of note are its higher DSi concentrations and $\delta^{30}Si_{DSi}$ signatures (Table 3; and lower f_{Si}; supporting information S2), relative to other Lake Baikal inflows (Figure 1 and Table 3). Although there are most likely differing weathering processes, land uses, and climate regimes within the catchment (which extends into Mongolia), variations to DSi concentrations and $\delta^{30}Si_{DSi}$ signatures are minimal. Indeed, DSi concentrations and $\delta^{30}Si_{DSi}$ compositions from sites located before and after the confluences of major lateral tributaries of the Selenga River at Novoselenginsk (Chikoi River), downstream of Dede-Sutoy (Khilok River) and in Ulan-Ude (River Uda), show no variation outside of analytical uncertainty to the Selenga River as a whole (Figure 1 and Table 3). This is in contrast to previous work highlighting that the mixing of waters from catchments, with differences in vegetation cover and land use, can alter $\delta^{30}Si_{DSi}$ at the subbasin level [*Delvaux et al.*, 2013]. The lack of variation in $\delta^{30}Si_{DSi}$ signatures is also notable given evidence of significant anthropogenic alteration in the landscape along the Selenga River, including industrial centers located close to the riverbanks at Ulan-Ude, Gusinoozersk, and Selenginsk, as well as mining activity and agriculture along the rivercourse [*Potemkina and Potemkin*, 2015; *Sorokovikova et al.*, 2015]. Indeed, landscape cultivation can lead to significant changes in soil and so water $\delta^{30}Si_{DSi}$, although this can be dependent on the time frame over which land has been cultivated [*Vandevenne et al.*, 2015]. In summary, while sampling of the Selenga River in Mongolia is required to confirm this, results from the Russian sector of the river suggest that anthropogenic influences on the Selenga River is, from a $\delta^{30}Si_{DSi}$ and DSi perspective, either (i) minimal, (ii) masked by the dilution with natural waters/silicon in the catchment, or (iii) undetectable due to anthropogenic sources of silicon having the same isotopic signature as Selenga River waters.

4.1.3. Cycling in the Selenga Delta

Wetland grasses/reeds, including *Phragmites*, which is found throughout the Selenga Delta, are considered to be silicon accumulators [*Struyf et al.*, 2009]. As such, rapid biogenic uptake by these organisms would be expected to have a significant impact on DSi concentrations and $\delta^{30}Si_{DSi}$ compositions in the Selenga Delta due to plant discrimination against ^{30}Si. Indeed, previous work has demonstrated significant changes in DSi and $\delta^{30}Si_{DSi}$ in wetlands due to biogenic uptake and phytolith formation [e.g., *Cockerton et al.*, 2013]. Except for samples from Korsakovo, discussed below, little variation in $\delta^{30}Si_{DSi}$ or DSi is observed across the Selenga Delta with values similar to the Selenga River (delta: $\overline{x} = +1.47‰$, 0.21 2 SD; river: +1.52‰, 0.29 2 SD, respectively) (Table 3). Dissolution of phytoliths from wetland vegetation can be extensive reaching up to 90% within 1 year after plants die [*Struyf et al.*, 2007]. While a lower pH can decrease phytoliths dissolution rate [*Fraysse et al.*, 2006], this issue is not relevant in the Selenga Delta where river water pH is ~8. Consequently, rapid recycling of phytoliths in the Selenga Delta may be replenishing the DSi pool and therefore maintaining $\delta^{30}Si_{DSi}$ signatures, between the river and delta region, at the same value. This balance, between uptake and dissolution, may be further reinforced by the restriction of significant biological uptake during the ice free period (March–October) [*Sorokovikova et al.*, 2006], compared to other deltaic regions around the world (e.g., the Nile) where seasonality and warmer temperatures permit increased productivity over the course of a year. This would lead to a net sink of silicon in these regions that is not balanced out by subsequent dissolution and release of silicon into the water column. The exception to this pattern in the Selenga Delta occurs at Korsakovo where DSi concentrations and $\delta^{30}Si_{DSi}$ signatures are higher than average (6.30 ppm, +1.77‰; Table 3). This was a heavily cattle-grazed site with waterlogged, grass-vegetated, riverbanks. It is possible that localized factors including the relative balance between weathering, nutrient uptake, and the impacts of grazing (e.g., waste and trampling of vegetation) may be altered sufficiently here to generate the observed change.

4.2. Si(OH)$_4$ Utilization/Export in Lake Baikal

Based on low (<0.05 ppm; Table 2) DSi concentrations in snow and ice, we assume negligible inputs of DSi to the lake from precipitation. Instead, nutrient inputs to the mixed layer in Lake Baikal are assumed to primarily derive from riverine inflow and upwelling from bottom waters, although we acknowledge that we have no

estimate of groundwater inputs which make up <4.5% of water inflow to the lake [*Seal and Shanks*, 1998] or the extent to which groundwater inputs may come from confined or unconfined reservoirs. Although lake waters ~1.8 km from the Selenga Delta outflow are strongly influenced by the relatively high DSi concentrations/low $\delta^{30}Si_{DSi}$ signatures of the Selenga River, values at all open water sites away from the shoreline (as well as samples close to the Khara-Murin and Vydrino River inflows) display lower DSi/higher $\delta^{30}Si_{DSi}$ that are similar to open lake water values. As such, while riverine inputs are likely to be the primary source of silicon to Lake Baikal (312 mmol m^{-2} yr^{-1}) [*Müller et al.*, 2005], these inputs are quickly diluted by preexisting waters in the lake, the majority of which lie below the MTM, with the export of 2700 mmol m^{-2} yr^{-1} into the deep waters of the south basin [*Müller et al.*, 2005]. With annual outflow of DSi through the Angara River (of 74 mmol m^{-2} yr^{-1}) and a silicon residence time of between 100 and 170 years [*Falkner et al.*, 1997; *Shimaraev and Domysheva*, 2004; *Müller et al.*, 2005] the $\delta^{30}Si_{DSi}$ signature of these deep waters (below 500 m), as indicated by their higher DSi concentration and lower $\delta^{30}Si$ (Table 1 and Figure 2) compositions, has been heavily impacted by in-lake biogeochemical cycling including (i) biomineralization, (ii) recycling/dissolution during sinking, and (iii) the export of silicon out of the system as organisms become incorporated into the sediment record. Accordingly, by comparing deepwater $\delta^{30}Si_{DSi}$ signatures (below 500 m) to river $\delta^{30}Si_{DSi}$ compositions, long-term rates of DSi export from surface waters and into the sediment record can be constrained (section 4.2.1). At the same time, at locations away from riverine/coastal inputs, mixed layer $\delta^{30}Si_{DSi}$ can be compared to deepwater $\delta^{30}Si_{DSi}$ to quantify seasonal trends of DSi utilization by diatoms with spatial and temporal variations providing insights into the homogeneity or heterogeneity of nutrient utilization across the lake (sections 4.2.2 and 4.2.3).

4.2.1. Long-Term DSi Utilization

Quantification of the silicon cycle in Lake Baikal can be performed by using an open system in which the pool of DSi is continually replenished by new inputs to the system. Mean deepwater (below 500 m) $\delta^{30}Si_{DSi}$ values for the north and south basins are similar ($\delta^{30}Si_{deep}$) at +1.77‰ and +1.71‰, respectively (Table 1 and Figure 2) (section 3.1.2). Within the context of examining long-term changes in silicon cycling in Lake Baikal, $\delta^{30}Si_{deep}$ can be expressed as a function of the $\delta^{30}Si_{DSi}$ signature of riverine inputs entering the lake prior to biomineralization ($\delta^{30}Si_{river}$), the fractionation factor (ε) between organisms and DSi, and the fraction of residual DSi that is not utilized during biomineralization (*f*):

$$\delta^{30}Si_{deep} = \delta^{30}Si_{river} - \varepsilon (1 - f) \qquad (2)$$

Diatoms dominate primary production in Lake Baikal, especially during spring and autumn overturn when deep waters replenish the mixed layer (surface) with waters enriched in DSi. While picoplankton also represent a significant proportion of primary productivity in Lake Baikal [*Fietz et al.*, 2005] no work has suggested that they accumulate significant levels of silicon, although evidence of this has been observed in marine picocyanobacteria [*Baines et al.*, 2012]. During the uptake of silicic acid, diatoms discriminate against the ^{30}Si isotope in favor of the lighter ^{28}Si isotope, causing the residual pool of DSi to become enriched in ^{30}Si. For diatoms, ε has often been estimated at approximately −1.1‰ in marine [e.g., *De La Rocha et al.*, 1997; *Milligan et al.*, 2004; *Varela et al.*, 2004; *Fripiat et al.*, 2011] and lake systems [e.g., *Alleman et al.*, 2005; *Opfergelt et al.*, 2011], although evidence of interspecies variations in ε is emerging [*Sutton et al.*, 2013]. Sediment traps from Lake Baikal suggest an ε of −1.61‰, which is applied in this study and used to obtain the results discussed below in order to look at spatial trends across the lake [*Panizzo et al.*, 2016]. For clarity, since the ε estimate of −1.61‰ for Lake Baikal is poorly constrained, involving assumptions about the mixing of deep and surface waters in spring [*Panizzo et al.*, 2016], we also present the results when using $\varepsilon = -1.1‰$ in Table 4. Using an ε of −1.1‰ alters the magnitude but does not change the spatial patterns of DSi utilization across the lake, which we are interested in this instance.

To calculate $\delta^{30}Si_{river}$ a weighted mass balance model of the fluvial input of silicon to the lake was conducted taking into account the relative annual discharge of each river flowing into the lake and their respective summer (August 2013) DSi concentrations and $\delta^{30}Si_{DSi}$ compositions. The use of summer-only data is justified by the lack of seasonal variation in the Selenga River (section 4.1.1) and the high proportion (>75%) of river inflow to the lake that occurs in the warmer months from May to September [*Afanasjev*, 1976]. Three further assumptions are made here. First, with sampled rivers accounting for 92% of the annual river inflow to Lake Baikal, we assume that the remaining 8% of inflows had a similar profile to the other rivers (Table 3). A

Table 4. Modeled Rates of Residual and Utilization DSi in Lake Baikal Using an ε of -1.61‰ (see Section 4.2 for Details)[a]

	$\varepsilon = -1.61$‰		$\varepsilon = -1.1$‰	
	Residual DSi (%)	Utilized DSi (%)	Residual DSi (%)	Utilized DSi (%)
Long-Term DSi Export Into Sediment Record				
South basin	80	20	70	30
North basin	76	24	65	35
Spring DSi utilization				
2003: South basin	64	36	48	52
2003: North basin	73	27	60	40
2013: South basin				
2013: BAIK13-1	22	78	−14	114
2013: BAIK13-4	52	48	30	70
2013: BAIK13-5	58	42	39	61
2013: BAIK13-7	53	47	31	69
2013: BAIK13-8	56	44	36	64
2013: BAIK13-9	71	29	58	42
2013: BAIK13-10	64	36	47	53
2013: BAIK13-11	9	91	−33	133
2013: Central basin				
2013: BAIK13-12	30	70	−2	102
2013: Maloe More (central basin)				
2013: BAIK13-13	57	43	38	62
2013: BAIK13-14	62	38	44	56
2013: North basin				
2013: BAIK13-16	49	51	26	74
2013: BAIK13-17	72	28	60	40
2013: BAIK13-18	84	16	77	23
2013: BAIK13-19	102	−2	102	−2
Autumn DSi Utilization: South Basin				
2012: BAIK13-1a	63	37	46	54
2012: BAIK13-1b	64	36	47	53
2012: BAIK13-1 (average)	64	36	47	53
2012: BAIK13-4	68	32	53	47
2012: BAIK13-5	63	37	46	54

[a]Model results when using an ε of -1.1‰ are also presented.

sensitivity test, in which the $\delta^{30}Si_{DSi}$ composition and DSi concentration of these unmeasured inflows varied between the maximum and minimum values recorded for other rivers, supports this assumption by only altering the weighted river $\delta^{30}Si$ and DSi by 0.04‰ and 0.09 ppm, respectively. Second, we assume that river DSi and $\delta^{30}Si_{DSi}$ signatures have remained unchanged over the last few centuries. While the lack of a clear anthropogenic impact on river $\delta^{30}Si_{DSi}$ in the Selenga River supports this assumption (section 4.1.2), the impact of a warmer climate over the last few decades in altering river $\delta^{30}Si_{DSi}$ signatures and DSi concentrations remains unknown. Reducing the inflows of the Selenga River by 10%, however, only alters the weighted river $\delta^{30}Si$ and DSi by 0.01‰ and 0.03 ppm, respectively. Finally, we assume that the weighted value for $\delta^{30}Si_{river}$ (+1.39‰) is representative of inflow to both the north and south basins. In practice, the $\delta^{30}Si_{river}$ value of +1.39‰ is strongly influenced by the Selenga River which contributes 62% of all riverine inflow to the lake, enters at the divide between the south and central basins, and has a higher isotopic composition (+1.47‰) and DSi (4.60 ppm) concentration than the other rivers (Table 3). Accordingly, the $\delta^{30}Si_{river}$ value of +1.39‰ may overestimate the true composition of riverine inflow to the north basin, although we assume that the impact of this over the long residence time of silicon in the lake (approximately 100–170 years) is low due to the mixing of waters between basins. Support for this can be found in $\delta^{18}O$ studies on Lake Baikal waters which show remarkably consistent values across the three basins despite considerable variation in the $\delta^{18}O$ composition of precipitation and river waters flowing into the lake [*Seal and Shanks*, 1998].

Since the 1950s between 75 and 80% of DSi entering Lake Baikal has remained either in the lake and/or been exported into the sediment record, with the remainder being exported via the Angara River outflow [*Votintzev et al.*, 1965; *Tarasova and Mescheryakova*, 1992; *Callender and Granina*, 1997]. Using an open

system model (equation (2)), our isotope measurements extended these studies by suggesting that over the last approximately 100–170 years 24% (north basin) and 20% (south basin) of all DSi entering Lake Baikal are exported into the sediment record (Table 4). The residual DSi (north basin = 76%, south basin = 80%) is either exported via the Angara River or retained in the water column where biogeochemical cycling transfers silicon into the deep waters where it is released during diatom dissolution. The latter is confirmed by the lower $\delta^{30}Si_{DSi}$ composition of deep, relative to surface, waters (Figure 2) and by a two box model in which only 54% (north basin) and 64% (south basin) of biogenic silica exported from the epilimnion are incorporated into the sediment record [*Müller et al.*, 2005], values not dissimilar to a global average DSi retention rate in lakes of 64% [*Frings et al.*, 2014b]. Of note here is the similarity between rates of DSi export between the north and south basins, in agreement with *Müller et al.* [2005], who also observed no significant difference in silicon fluxes between the two basins. These results are of importance in the light of *Müller et al.* [2005], who were unable to fully balance south basin modeled DSi fluxes (e.g., hypolimnion concentrations were too low), which the authors attributed to be a response to a "Melosira" diatom bloom event. Here we are able to show support to the previous estimations and more importantly, we provide enhanced spatial representation of DSi utilization across all three main basins at Lake Baikal (Table 4; section 4.2.2). This application is further supported by the novel estimation of Lake Baikal diatom fractionation factors, which are applied here to obtain more accurate estimates of DSi utilization [*Panizzo et al.*, 2016].

4.2.2. Spring DSi Utilization

With an open system model, mixed layer $\delta^{30}Si_{DSi}$ from Lake Baikal ($\delta^{30}Si_{mixed}$) can be used to assess the magnitude of seasonal DSi utilization in Lake Baikal and by assuming that the primary source of DSi to the mixed layer at open water sites is deep water ($\delta^{30}Si_{deep}$) rather than riverine inputs which, as discussed above, are quickly diluted/mixed with preexisting waters in the lake:

$$\delta^{30}Si_{deep} = \delta^{30}Si_{mixed} - \varepsilon\,(1-f) \tag{3}$$

By using summer $\delta^{30}Si_{mixed}$ values from 2003 (sampled water depth = 10 m in south basin; 5 m in north basin) and 2013 (sampled water depth = 1 m), the magnitude of spring DSi utilization can be calculated by comparison to the respective value of $\delta^{30}Si_{deep}$ for the north and south basins (equation (3) and Table 4). Deeper waters in the MTM were not used to derive $\delta^{30}Si_{mixed}$ to ensure that samples were not affected by diatom dissolution during sinking, which releases silicon back into the water column. Using equation (3) to calculate mixed layer DSi utilization assumes that (1) seasonal overturning prior to the onset of the spring and autumn diatom blooms resets the value of $\delta^{30}Si_{mixed}$ to that of $\delta^{30}Si_{deep}$ and (2) 2003 $\delta^{30}Si_{deep}$ values can be compared to 2013 $\delta^{30}Si_{mixed}$ data; i.e., $\delta^{30}Si_{deep}$ has not changed between 2003 and 2013, supported by the approximately 100–170 year residency time of silicon in Lake Baikal [*Falkner et al.*, 1997; *Shimaraev and Domysheva*, 2004]. The first assumption does not account for the mixing of upwelled deep water with preexisting winter surface waters, the relative proportions of which remain unconstrained due to the complexity of mixing in the lake [*Shimaraev et al.*, 2012]. Peak fluxes of diatoms, however, occur in May [*Panizzo et al.*, 2016] when overturning would have likely caused the mixed layer to be dominated by upwelled deep waters, justifying the use of $\delta^{30}Si_{deep}$ in equation (3). Using a weighted deep and winter surface water value in equation (3) for $\delta^{30}Si_{mixed}$ would have altered the estimated magnitude of DSi utilization, but not spatial patterns across the lake, which this manuscript focuses on.

Annual diatom blooms peak in the spring months and $\delta^{30}Si_{mixed}$ data from July 2003 indicate that 27% and 36% of available DSi were utilized in the north and south basins, respectively, during the spring 2003 season (Table 4). The $\delta^{30}Si_{mixed}$ data from August 2013, however, show considerable variability in rates of DSi utilization across the lake during the 2013 spring bloom ($\overline{x}$ = 44%, 1 SD = 23‰, range = 91% to −2%) (Table 4). In the south basin, the rates of DSi utilization range from 29 to 91% ($\overline{x}$ = 52%, 1 SD = 21‰), in the central basin including Maloe More from 38 to 70% ($\overline{x}$ = 50%, 1 SD = 17‰), while in the north basin values are noticeably lower ranging from 51% to −2% ($\overline{x}$ = 32%, 1 SD = 17‰). The values of <0% (BAIK13-19: north basin) can be attributed by using a $\delta^{30}Si_{deep}$ value from 2003 and/or the sensitivity of equation (3) to estimates of $\delta^{30}Si_{deep}$. For example, varying north basin $\delta^{30}Si_{deep}$ by only 0.03‰ alters the modeled value at BAIK13-19 to >0%.

These results from the spring 2003 and 2013 bloom seasons contrast with the long-term estimate of silicon export into the sediment record (section 4.2.1) by revealing significant spatial and seasonal variabilities in rates of mixed layer DSi utilization across the lake. Intriguingly, the rates in Maloe More are similar to the

central and south basins despite concern over anthropogenic impacts (e.g., nutrient loading and pollution) upon phytoplankton communities in this sector of the lake [*Timoshkin et al.*, 2016]. However, the lower rates of utilization in the north basin relative to the central and south basins for both the 2003 and 2013 spring blooms contradict the previously mentioned evidence of similar silicon fluxes between the two basins. There is no overriding feature to explain the significant spatial variability across the lake, and without information for other years it is not possible to examine the extent to which recent warming and reductions in ice cover are affecting changes in DSi utilization. However, long-term reductions in lake DSi have been documented throughout the water column from 1993 to 2001 [*Shimaraev and Domysheva*, 2002, 2004] with reduced development of phytoplankton in the north basin relative to the central and south basins [*Popovskaya et al.*, 2015]. Further controls of nutrient availability upon diatom biomass have been highlighted by *Jewson et al.* [2008], where phosphate availability in the north basin remained above the induction threshold (23 $\mu g\,L^{-1}$ P-PO$_4$) needed to promote successful *Aulacoseira skvortzowii* resting stage formation, thereby reducing cell regeneration and their subsequent concentrations (e.g., in 1998, 1999, and 2003) when compared to the south and central basins. Another notable difference between 2003 and 2013 is the occurrence of a "Melosira event," a phenomena occurring every 3–4 years in which populations of the diatom *Aulacoseira baicalensis* increase by up to 100-fold. Unlike 2003, 2013 was a Melosira year although the bloom of *A. baicalensis* occurred much later than usual and extended into July/August. While much remains unknown about the causes [*Katz et al.*, 2015] and spatial variability of these events across the lake, a Melosira event could explain the large spatial variations in DSi utilization for the spring 2013 bloom. For example, data in *Popovskaya et al.* [2015] show that Melosira events coincide with significant biomass increases in the south and central basins, which would account for the exceptionally high rates of DSi utilization at sites BAIK13-12 (70% utilization) and BAIK13-1 (78% utilization) in 2013, whereas biomass changes in the north basin are generally much smaller in a Melosira event year (as per the estimated DSi utilization: BAIK13-16, etc; Table 4). The long-term effects of these *A. baicalensis* blooms upon Si availability have been highlighted by *Jewson and Granin* [2015], where following high diatom abundance years (e.g., in the year 1997) [*Shimaraev and Domysheva*, 2004; *Jewson et al.*, 2010] a net loss of up to 17% of total DSi is exported from the surface system (as sinking diatoms) and is not replaced by autumn overturn ahead of the following spring bloom (namely, switching to a DSi limited system the following year).

4.2.3. Autumn DSi Utilization

Similar to the spring bloom, $\delta^{30}Si_{mixed}$ data from February/March 2013 prior to the onset of the spring overturning/diatom bloom can be used to assess DSi usage in the preceding autumn bloom (i.e., autumn 2012 A.D.). This assumes that no mixing of surface and deepwater masses has occurred over the winter months following the end of the autumn bloom. With sampling conducted from the ice, we calculate $\delta^{30}Si_{mixed}$ at each site as the average $\delta^{30}Si_{DSi}$ composition for waters between the surface and 180 m depth (Table 2) as, during periods of ice cover, the upper layers of the water column reach a MTM at approximately 150–250 m [*Shimaraev et al.*, 1994] and no biological productivity was occurring in the lake at the time of sampling. South basin winter (February/March 2013) $\delta^{30}Si_{mixed}$ from sites BAIK13-1, BAIK13-4, and BAIK13-5 indicate that in the 2012 autumn bloom 36%, 32%, and 37% of available DSi were utilized, respectively (Table 4). The lower rates of autumn 2012 DSi utilization, relative to the spring 2013 bloom, reflect the reduced levels of diatom productivity associated with the autumn bloom, which are typically 2 to 8 times lower but up to 100 times lower in some years [*Popovskaya*, 2000; *Popovskaya et al.*, 2015] with the similarity of these autumn estimates in sharp contrast to the more variable values for the spring 2013 bloom. While values at BAIK13-4 are lower than at BAIK13-1 and BAIK13-5, replicate sampling at BAIK13-1 9 days apart confirms the robustness of the results with DSi utilization rates of 37% and 36%, respectively (BAIK13-1a and BAIK13-1b; Table 4).

5. Conclusions

This study represents the first use of $\delta^{30}Si$ in Lake Baikal to provide insights into both the long-term export of DSi into the sediment record and seasonal variations in mixed layer DSi utilization following the onset of spring and autumn overturning. Over the last century around a quarter of all DSi entering the lake has ultimately been exported into the sediment record by diatom blooms in the lake. However, $\delta^{30}Si_{mixed}$ data from 2003 and 2013 show that this long-term trend is superimposed by a significant degree of temporal and spatial variabilities, highlighting the complexity of this lake system.

Questions remain about the extent to which both local and distal anthropogenic pressures may be influencing wider biogeochemical cycling in Lake Baikal. The relative homogeneity of $\delta^{30}Si_{DSi}$ along Lake Baikal's largest inflow, the Selenga River, may suggest that any anthropogenic alteration in the catchment is having minimal impacts on the silicon isotopic signature and DSi concentrations in the river. Similarly, the lack of change through the Selenga Delta also suggests that the uptake and recycling of silicon by vegetation/phytoliths are in balance. Further work using $\delta^{30}Si$ analyses on diatoms preserved in sediments from the lake are now required to investigate temporal changes in DSi utilization over the last 2000 years in order to fully constrain and trace natural versus human impacts on biogeochemical cycling in the lake.

This research emphasizes the temporal and spatial variabilities in DSi export in Lake Baikal and highlights the importance to fully constrain continental Si cycling [e.g., *Frings et al.*, 2016] in such large-scale drainage basins, as a means to estimates DSi fluxes to the oceanic biogeochemical pump. This is of even greater importance for large river catchments, such as Lake Baikal, which are increasingly demonstrating alterations to lacustrine biogeochemical cycling as a response to anthropogenic nutrient loading and climate change. Such implications of a move away from a steady state interpretation for the continental Si cycle over recent decades has already been highlighted [*Frings et al.*, 2014b], which can have significant impacts upon the oceanic Si cycle.

References

Afanasjev, A. N. (1976), *The Water Resources and Water Balance of Lake Baikal Basin*, Nauka, Novosibirsk, Russia.

Alleman, L. Y., D. Cardinal, C. Cocquyt, P.-D. Plisnier, J. P. Descy, I. Kimirei, D. Sinyinza, and L. Andre (2005), Silicon isotopic fractionation in Lake Tanganyika and its main tributaries, *J. Great Lakes Res.*, *31*, 509–519.

Baines, S. B., B. S. Twining, M. A. Brzezinski, J. W. Krause, S. Vogt, D. Assael, and H. McDaniel (2012), Significant silicon accumulation by marine picocyanobacteria, *Nat. Geosci.*, *5*, 886–891.

Callender, E., and L. Granina (1997), Geochemical mass balance of major elements in Lake Baikal, *Limnol. Oceanogr.*, *42*, 148–155.

Cardinal, D., L. Y. Alleman, J. de Jong, K. Ziegler, and L. Andre (2003), Isotopic composition of silicon measured by multicollector plasma source mass spectrometry in dry plasma mode, *J. Anal. At. Spectrom*, *18*, 213–218.

Cardinal, D., L. Y. Alleman, F. Dehairs, N. Savoye, T. W. Trull, and L. André (2005), Relevance of silicon isotopes to Si-nutrient utilization and Si-source assessment in Antarctic waters, *Global Biogeochem. Cycles*, *19*, GB2007, doi:10.1029/2004GB002364.

Cardinal, D., J. Gaillardet, H. J. Hughes, S. Opfergelt, and L. André (2010), Contrasting silicon isotope signatures in rivers from the Congo Basin and the specific behaviour of organic-rich waters, *Geophys. Res. Lett.*, *37*, L12403, doi:10.1029/2010GL043413.

Ciesielski, T., M. V. Pastukhov, P. Fodor, Z. Bertenyi, J. Namiesnik, and P. Szefer (2006), Relationships and bioaccumulation of chemical elements in the Baikal seal (Phoca sibirica), *Environ. Pollut.*, *139*, 372–384.

Cockerton, H. E., F. A. Street-Perrott, M. J. Leng, P. A. Barker, M. S. A. Horstwood, and V. Pashley (2013), Stable-isotope (H, O, and Si) evidence for seasonal variations in hydrology and Si cycling from modern waters in the Nile Basin: Implications for interpreting the Quaternary record, *Quat. Sci. Rev.*, *66*, 4–21.

Conley, D. J. (2002), Terrestrial ecosystems and the global biogeochemical silica cycle, *Global Biogeochem. Cycles*, *16*(4), 68-1–68-8, doi:10.1029/2002GB001894.

Conley, D. J., and J. C. Carey (2015), Silica cycling over geologic time, *Nat. Geosci.*, *8*, 431–432.

De La Rocha, C. L., M. A. Brzezinski, and M. J. DeNiro (1997), Fractionation of silicon isotopes by marine diatoms during biogenic silica formation, *Geochim. Cosmochim. Acta*, *61*, 5051–5056.

De La Rocha, C. L., M. A. Brzezinski, and M. J. DeNiro (2000), A first look at the distribution of the stable isotopes of silicon in natural waters, *Geochim. Cosmochim. Acta*, *64*, 2467–2477.

Delvaux, C., D. Cardinal, V. Carbonnel, L. Chou, H. J. Hughes, and L. André (2013), Controls on riverine $\delta^{30}Si$ signatures in a temperate watershed under high anthropogenic pressure (Scheldt-Belgium), *J. Mar. Syst.*, *128*, 40–51.

Digital Chart of the World (2007), DCW hydrological data of the Baikal region; Deutsches GeoForschungsZentrum GFZ, doi:10.1594/GFZ.SDDB.1208.

Ding, T., D. Wan, C. Wang, and F. Zhang (2004), Silicon isotope compositions of dissolved silicon and suspended matter in the Yangtze River, China, *Geochim. Cosmochim. Acta*, *68*, 205–216.

Ding, T. P., J. F. Gao, S. H. Tian, H. B. Wang, and M. Li (2011), Silicon isotopic composition of dissolved silicon and suspended particulate matter in the Yellow River, China, with implications for the global silicon cycle, *Geochim. Cosmochim. Acta*, *75*, 6672–6689.

Edmond, J. M., M. R. Palmer, C. I. Measures, B. Grant, and R. F. Stallard (1995), The fluvial geochemistry and denudation rate of the Guayana Shield in Venezuela, Colombia, and Brazil, *Geochim. Cosmochim. Acta*, *59*, 3301–3325.

Engström, E., I. Rodushkin, J. Ingri, D. C. Baxter, F. Ecke, H. Osterlund, and B. Ohlander (2010), Temporal isotopic variations of dissolved silicon in a pristine boreal river, *Chem. Geol.*, *271*, 142–152.

Falkner, K. K., M. Church, C. Measures, G. LeBaron, D. Touron, C. Jeandel, M. C. Stordal, G. A. Gill, R. A. Mortlock, and P. Froelich (1997), Minor and major element chamistry of Lake Baikal, its tributaries, and surrounding hot springs, *Limnol. Oceanogr.*, *42*, 329–345.

Fefelov, I. V. (2001), Comparative breeding ecology and hybridization of Eastern and Western Marsh Harriers Circus spilonotus and C-aeruginosus in the Baikal Region of Eastern Siberia, *Ibis*, *143*, 587–592.

Fietz, S., M. Sturm, and A. Nicklisch (2005), Flux of lipophilic photosynthetic pigments to the surface sediments of Lake Baikal Global Planet, *Change*, *46*, 29–44.

Fontorbe, G., C. L. De La Rocha, H. J. Chapman, and M. J. Bickle (2013), The silicon isotopic composition of the Ganges and its tributaries, *Earth Planet. Sci. Lett.*, *381*, 21–30.

Fraysse, F., O. S. Pokrovsky, J. Schott, and J.-D. Meunier (2006), Surface properties, solubility and dissolution kinetics of bamboo phytoliths, *Geochim. Cosmochim. Acta*, *70*, 1939–1951.

Frings, P. J., et al. (2014a), Tracing silicon cycling in the Okavango Delta, a sub-tropical flood-pulse wetland using silicon isotopes, *Geochim. Cosmochim. Acta*, *142*, 132–148.

Frings, P. J., W. Clymans, E. Jeppesen, T. L. Lauridsen, E. Struyf, and D. J. Conley (2014b), Lack of steady-state in the global biogeochemical Si cycle: Emerging evidence from lake Si sequestration, *Biogeochemistry*, *117*, 255–277.

Frings, P. J., W. Clymans, G. Fontorbe, W. Gray, G. J. Chakrapani, D. J. Conley, and C. L. De La Rocha (2015), Silicate weathering in the Ganges alluvial plain, *Earth Planet. Sci. Lett.*, *427*, 136–148.

Frings, P. J., W. Clymans, G. Fontorbe, C. L. De La Rocha, and D. J. Conley (2016), The continental Si cycle and its impact on the ocean Si isotope budget, *Chem. Geol.*, *425*, 12–36.

Fripiat, F., A. J. Cavagna, F. Dehairs, S. Speich, L. André, and D. Cardinal (2011), Silicon pool dynamics and biogenic silica export in the Southern Ocean inferred from Si-isotopes, *Ocean Sci.*, *7*, 533–547.

Fryer, G. (1991), Comparative aspects of adaptive radiation and speciation in Lake Baikal and the great rift lakes of Africa, *Hydrobiologia*, *211*, 137–146.

Georg, R. B., B. C. Reynolds, M. Frank, and A. N. Halliday (2006a), Mechanisms controlling the silicon isotopic compositions of river waters, *Earth Planet. Sci. Lett.*, *249*, 290–306.

Georg, R. B., B. C. Reynolds, M. Frank, and A. N. Halliday (2006b), New sample preparation techniques for the determination of Si isotopic compositions using MC-ICPMS, *Chem. Geol.*, *235*, 95–104.

Georg, R. B., B. C. Reynolds, A. J. West, K. W. Burton, and A. N. Halliday (2007), Silicon isotope variations accompanying basalt weathering in Iceland, *Earth Planet. Sci. Lett.*, *261*, 476–490.

Gronskaya, T. P., and T. E. Litova (1991), Kratkaya harakteristika vodnogo balansa ozera Baikal za period 1962–1988 (Short characteristics of the water balance of Lake Baikal during 1962–1988), Gidrometeoizdsat, Leningrad.

Hampton, S. E., L. R. Izmest'eva, M. V. Moore, S. L. Katz, B. Dennis, and E. A. Silow (2008), Sixty years of environmental change in the world's largest freshwater lake - Lake Baikal, Siberia, *Global Change Biol.*, *14*, 1947–1958.

Hampton, S. E., D. K. Gray, L. R. Izmest'eva, M. V. Moore, and T. Ozersky (2014), The rise and fall of plankton: Long-term changes in the vertical distribution of algae and grazers in Lake Baikal, Siberia, *Plos One*, *2*, e88920, doi:10.1371/journal.pone.0088920.

Hohmann, R., R. Kipfer, F. Peeters, G. Piepke, D. M. Imboden, and M. N. Shimaraev (1997), Deep-water renewal in Lake Baikal, *Limnol. Oceanogr.*, *42*, 841–855.

Hughes, H. J., F. Sondag, C. Cocquyt, A. Laraque, A. Pandi, L. Andre, and D. Cardinal (2011a), Effect of seasonal biogenic silica variations on dissolved silicon fluxes and isotopic signatures in the Congo River, *Limnol. Oceanogr.*, *56*, 551–561.

Hughes, H. J., C. Delvigne, M. Korntheuer, J. de Jong, L. André, and D. Cardinal (2011b), Controlling the mass bias introduced by anionic and organic matrices in silicon isotopic measurements by MC-ICP-MS, *J. Anal. At. Spectrom*, *26*, 1892–1896.

Hughes, H. J., S. Bouillon, L. André, and D. Cardinal (2012), The effects of weathering variability and anthropogenic pressures upon silicon cycling in an intertropical watershed (Tana River, Kenya), *Chem. Geol.*, *308*, 18–25.

Hughes, H. J., F. Sondag, R. V. Santos, L. André, and D. Cardinal (2013), The riverine silicon isotope composition of the Amazon Basin, *Geochim. Cosmochim. Acta*, *121*, 637–651.

Izmest'eva, L. R., M. V. Moore, S. E. Hampton, C. J. Ferwerda, D. K. Gray, K. H. Woo, H. V. Pislegina, L. S. Krashchuk, S. V. Shimaraeva, and E. A. Silow (2016), Lake-wide physical and biological trends associated with warming in Lake Baikal, *J. Great Lakes Res.*, *42*, 6–17.

Jewson, D. H., and N. G. Granin (2015), Cyclical size change and population dynamics of a planktonic diatom, *Aulacoseira baicalensis*, in Lake Baikal, *Eur. J. Phycol.*, *50*, 1–19.

Jewson, D. H., N. G. Granin, A. A. Zhdanov, L. A. Gorbunova, N. A. Bondarenko, and R. Y. Gnatovsky (2008), Resting stages and ecology of the planktonic diatom *Aulacoseira skvortzowii* in Lake Baikal, *Limnol. Oceanogr.*, *53*, 1125–1136.

Jewson, D. H., N. G. Granin, A. A. Zhdanov, and R. Y. Gnatovsky (2009), Effect of snow depth on under-ice irradiance and growth of *Aulacoseira baicalensis* in Lake Baikal, *Aquat. Ecol.*, *43*, 673–679.

Jewson, D. H., N. G. Granin, A. A. Zhdarnov, L. A. Gorbunova, and R. Y. Gnatovsky (2010), Vertical mixing, size change and resting stage formation of the planktonic diatom *Aulacoseira baicalensis*, *Eur. J. Phycol.*, *45*, 354–364.

Johnson, C. M., B. L. Beard, and F. Albarède (2004), Overview and general concepts, in *Geochemistry of nontraditional stable isotopes, Reviews in Mineralogy and Geochemistry*, vol. 55, edited by C. M. Johnson, B. L. Beard, and F. Albarède, pp. 1–24, Mineralogical Society of America, Chantilly, Va.

Katz, S. L., L. R. Izmest'eva, S. E. Hampton, T. Ozersky, K. Shchapov, M. V. Moore, S. V. Shimaraeva, and E. A. Silow (2015), The "Melosira years" of Lake Baikal: Winter environmental conditions at ice onset predict under-ice algal blooms in spring, *Limnol. Oceanogr.*, *60*, 1950–1964.

Killworth, P. D., E. C. Carmack, R. F. Weiss, and R. Matear (1996), Modeling deep-water renewal in Lake Baikal, *Limnol. Oceanogr.*, *41*, 1521–1538.

Kipfer, R., and F. Peeters (2000), Some speculations on the possibility of changes in deep-water renewal in Lake Baikal and their consequences, in *Lake Baikal*, edited by K. Minoura, pp. 273–280, Elsevier, Netherlands.

Laruelle, G. G., et al. (2009), Anthropogenic perturbations of the silicon cycle at the global scale: key role of the land-ocean transition, *Global Biogeochem. Cycles*, *23*, GB4031, doi:10.1029/2008GB003267.

Lydolph, P. E. (1977), *Geography of the USSR*, Elsevier, The Hague.

Martin-Jézéquel, V., M. Hildebrand, and M. A. Brzezinski (2000), Silicon metabolism in daitoms: Implications for growth, *J. Phycol.*, *36*, 821–840.

Mavromatis, V., T. Rinder, A. S. Prokushkin, O. S. Pokrovsky, M. A. Korets, J. Chmeleff, and E. H. Oelkers (2016), The effect of permafrost, vegetation, and lithology on Mg and Si isotope composition of the Yenisey River and its tributaries at the end of the spring flood, *Geochim. Cosmochim. Acta*, *191*, 32–46.

Milligan, A. J., D. E. Varela, M. A. Brzezinski, and F. M. M. Morel (2004), Dynamics of silicon metabolism and silicon isotopic discrimination in a marine diatom as a function of pCO_2, *Limnol. Oceanogr.*, *49*, 322–329.

Müller, B., M. Maerki, M. Schmid, E. G. Vologina, B. Wehrli, A. Wuest, and M. Sturm (2005), Internal carbon and nutrient cycling in Lake Baikal: Sedimentation, upwelling, and early diagenesis, *Global Planet. Change*, *46*, 101–124.

Oelze, M., J. A. Schuessler, and F. von Blackenburg (2016), Mass bias stabilization by Mg doping for Si stable isotope analysis by MC-ICP-MS, *J. Anal. At. Spectrom*, *31*, 2094–2100.

Opfergelt, S., and P. Delmelle (2012), Silicon isotopes and continental weathering processes: Assessing controls on Si transfer to the ocean, *C. R. Geosci.*, *344*, 723–738.

Opfergelt, S., E. S. Eiriksdottir, K. W. Burton, A. Einarsson, C. Siebert, S. R. Gislason, and A. N. Halliday (2011), Quantifying the impact of freshwater diatom productivity on silicon isotopes and silicon fluxes: Lake Myvatn, Iceland, *Earth Planet. Sci. Lett.*, *305*, 73–82.

Opfergelt, S., K. W. Burton, P. A. E. Pogge von Strandmann, S. R. Gislason, and A. N. Halliday (2013), Riverine silicon isotope variations in glaciated basaltic terrains: Implications for the Si delivery to the ocean over glacial-interglacial intervals, *Earth Planet. Sci. Lett.*, *369-370*, 211–219.

Panizzo, V. N., G. E. A. Swann, A. W. Mackay, E. Vologina, M. Sturm, V. Pashley, and M. S. A. Horstwood (2016), Insights into the transfer of silicon isotopes into the sediment record, *Biogeosciences*, *13*, 147–157.

Pokrovsky, O. S., B. C. Reynolds, A. S. Prokushkin, J. Schott, and J. Viers (2013), Silicon isotope variations in Central Siberian rivers during basalt weathering in permafrost-dominated larch forests, *Chem. Geol.*, *355*, 103–116.

Popovskaya, G. I. (2000), Ecological monitoring of phytoplankton in Lake Baikal, *Aquat. Ecosyst. Health Manage.*, *3*, 215–225.

Popovskaya, G. I., M. V. Usol'tseva, V. M. Domysheva, M. V. Sakirko, V. V. Blinov, and T. V. Khodzher (2015), The spring phytoplankton in the pelagic zone of Lake Baikal during 2007–2011, *Geogr. Nat. Resour.*, *36*, 253–262.

Potemkina, T. G., and V. L. Potemkin (2015), Sediment load of the main rivers of Lake Baikal in a changing environment (east Siberia, Russia), *Quat. Int.*, *380–381*, 342–349.

QGIS Development Team (2016), QGIS Geographic Information System. Open Source Geospatial Foundation Project. [Available at http://qgis.osgeo.org.]

Ravens, T. M., O. Kocsis, A. Wuest, and N. Granin (2000), Small-scale turbulence and vertical mixing in Lake Baikal, *Limnol. Oceanogr.*, *45*, 159–173.

Reynolds, B. C., et al. (2007), An inter-laboratory comparison of Si isotope reference materials, *J. Anal. At. Spectrom*, *22*, 561–568.

Rudnick, R. L., and S. Gao (2003), 3.01—Composition of the continental crust, in *Treatise on Geochemistry*, edited by H. D. Holland and K. K. Turekian, pp. 1–64, Oxford, Pergamon.

Savage, P. S., R. B. Georg, H. M. Williams, and A. N. Halliday (2013), The silicon isotope composition of the upper continental crust, *Geochim. Cosmochim. Acta*, *109*, 384–399.

Seal, R., and W. Shanks (1998), Oxygen and hydrogen isotope systematics of Lake Baikal, Siberia: Implications for paleoclimate studies, *Limnol. Oceanogr.*, *43*, 1251–1261.

Sherstyankin, P. P., S. P. Alekseev, A. M. Abramov, K. G. Stavrov, M. De Batist, R. Hus, M. Canals, and J. L. Casamor (2006), Bathymetric computer-based map of Lake Baikal, *Dokl. Akad. Nauk*, *408*, 102–107.

Shimaraev, M., V. Verbolov, N. G. Granin, and P. Sherstyankin (1994), *Physical Limnology of Lake Baikal: A Review. Baikal International Centre for Ecological Research (BOOK)*, pp. 1–89, BICER, Irkutsk and Okayama.

Shimaraev, M. N., and N. G. Granin (1991), Temperature stratification and the mechanisms of convection in Lake Baikal, *Dokl. Akad. Nauk*, *321*, 381–385.

Shimaraev, M. N., and V. M. Domysheva (2002), Dynamics of dissolved silica in Lake Baikal, *Dokl. Earth Sci.*, *387A*, 1075–1078.

Shimaraev, M. N., and V. M. Domysheva (2004), Climate and long-term silica dynamics in Lake Baikal, *Russ. Geol. Geophys.*, *45*, 310–316.

Shimaraev, M. N., and V. M. Domysheva (2013), Trends in hydrological and hydrochemical processes in Lake Baikal under conditions of modern climate change, in *Climatic Change and Global Warming of Inland Waters: Impacts and Mitigation for Ecosystems and Societies*, 1st ed., edited by C. R. Goldman, M. Kumagai, and R. D. Robarts, pp. 43–66, John Wiley, Oxford, U. K.

Shimaraev, M. N., N. G. Granin, and A. A. Zhdanov (1993), Deep ventilation of Lake Baikal waters due to spring thermal bars, *Limnol. Oceanogr.*, *38*, 1068–1072.

Shimaraev, M. N., E. S. Troitskaya, V. V. Blinov, V. G. Ivanov, and R. Y. Gnatovskii (2012), Upwellings in Lake Baikal, *Dokl. Akad. Nauk*, *442*, 696–700.

Sorokovikova, L. M., G. I. Popovskaya, V. N. Sinyukovich, I. V. Tomberg, N. V. Bashenkhaeva, and N. A. Tashlykova (2006), Water chamistry and phytoplankton in water bodies in the Selenga River's delta under ice cover, *Water Resour.*, *33*, 321–328.

Sorokovikova, L. M., V. N. Sinyukovich, I. V. Tomberg, I. I. Marinaite, and T. V. Khodzher (2015), Assessing the water quality in the tributary streams of Lake Baikal from chemical parameters, *Geogr. Nat. Resour.*, *36*, 37–45.

Stallard, R. (1980), Major element geochemistry of the Amazon River system. PhD thesis, Massachusetts Inst. Technol.

Straškrábová, V., L. R. Izmest'yeva, E. A. Maksimova, S. Fietz, J. Nedoma, J. Borovec, G. I. Kobanova, E. V. Shchetinina, and E. V. Pislegina (2005), Primary production and microbial activity in the euphotic zone of Lake Baikal (Southern Basin) during late winter, *Global Planet. Change*, *46*, 57–73.

Street-Perrott, F. A., and P. A. Barker (2008), Biogenic silica: A neglected component of the coupled global continental biogeochemical cycles of carbon and silicon, *Earth Surf. Process. Landf.*, *33*, 1436–1457.

Struyf, E., S. Van Damme, B. Gribsholt, K. Bal, O. Beauchard, J. J. Middelburg, and P. Meire (2007), Phragmites australis and silica cycling in tidal wetlands, *Aquat. Bot.*, *87*, 134–140.

Struyf, E., A. Smis, S. Van Damme, P. Meire, and D. J. Conley (2009), The global biogeochemical silicon cycle, *Silicon*, *1*, 207–213.

Sun, X. L., P. S. Andersson, C. Humborg, M. Pastuszak, and C. M. Morth (2013), Silicon isotope enrichment in diatoms during nutrient-limited blooms in a eutrophied river system, *J. Geochem. Explor.*, *132*, 173–180.

Sutton, J. N., D. E. Varela, M. A. Brzezinski, and C. P. Beucher (2013), Species-dependent silicon isotope fractionation by marine diatoms, *Geochim. Cosmochim. Acta*, *104*, 300–309.

Swiercz, S. (2007), Lake catchment; Deutsches GeoForschungsZentrum GFZ, doi:10.1594/GFZ.SDDB.1210.

Tarasova, E. N., and A. I. Mescheryakova (1992), *Modern State of Hydrochemical Regime of Lake Baikal (in Russian)*, Nauka, Novosibirsk, Russia.

Timoshkin, O. A. (1997), Biodiversity of Baikal fauna: State-of-the-art (Preliminary analysis), in *New Scope on the Boreal Ecosystems in East Siberia. Proceedings of the International Symposium, Kyoto, Nov. 23–25 1994, (DIWPA Ser. No.2)*, edited by E. Wada et al., pp. 35–76, The Siberian Branch of the Russian Academy of Sciences Press, Novosibirsk, Russia.

Timoshkin, O. A., et al. (2016), Rapid ecological change in the coastal zone of Lake Baikal (East Siberia): Is the site of the world's greatest freshwater biodiversity in danger?, *J. Great Lakes Res.*, *42*, 487–497.

Todd, M. C., and A. W. Mackay (2003), Large-scale climatic controls on Lake Baikal ice cover, *J. Clim.*, *16*, 3186–3199.

Tréguer, P., and P. Pondaven (2000), Silica control of carbon dioxide, *Nature*, *406*, 358–359.

Tréguer, P., D. M. Nelson, A. J. van Bennekom, D. J. DeMaster, A. Leynaert, and B. Queguiner (1995), The silica balance in the world ocean: A re-estimate, *Science*, *268*, 375–379.

Tréguer, P. J., and C. L. De La Rocha (2013), The world ocean silica cycle, *Ann. Rev. Mar. Sci.*, *5*, 477–501.

Troitskaya, E., V. Blinov, V. Ivanov, A. Zhdanov, R. Gnatovsky, E. Sutyrina, and M. Shimaraev (2014), Cyclonic circulation and upwelling in Lake Baikal, *Aquat. Sci.*, *77*(2), 171–182.

Vandevenne, F. I., et al. (2015), Landscape cultivation alters δ^{30}Si signature in terrestrial ecosystems, *Sci. Rep.*, *5*, 7732, doi:10.1038/srep07732.

Varela, D. E., C. J. Pride, and M. A. Brzezinski (2004), Biological fractionation of silicon isotopes in Southern Ocean surface waters, *Global Biogeochem. Cycles*, *18*, GB1047, doi:10.1029/2003GB002140.

Votintzev, K. K., I. V. Glazunov, and A. P. Tolmachyova (1965), *Hydrochemistry of Rivers of Lake Baikal basin*, Nauka, Moscow.

Weiss, R. F., E. C. Carmack, and V. M. Koropalov (1991), Deep-water renewal and biological production in Lake Baikal, *Nature*, *349*, 665–669.

Wessel, P., and W. Smith (2007), GMT drainage pattern of the Baikal region; Deutsches GeoForschungsZentrum GFZ, doi:10.1594/GFZ. SDDB.1209.

Wüest, A., T. M. Ravens, N. G. Granin, O. Kocsis, M. Schurter, and M. Sturm (2005), Cold intrusions in Lake Baikal: Direct observational evidence for deep-water renewal, *Limnol. Oceanogr.*, *50*, 184–196.

Ziegler, K., O. A. Chadwick, M. A. Brzezinski, and F. F. Kelly (2005a), Natural variations of delta Si-30 ratios during progressive basalt weathering, Hawaiian Islands, *Geochim. Cosmochim. Acta*, *69*, 4597–4610.

Ziegler, K., O. A. Chadwick, A. F. White, and M. A. Brzezinski (2005b), (DSi)-Si-30 systematics in a granitic saprolite, Puerto Rico, *Geology*, *33*, 817–820.